

Ethylene Polymerization by Sterically Crowded Palladium(II) Complexes that Contain Bis(heterocycle)methane Ligands

Christopher T. Burns and Richard F. Jordan*

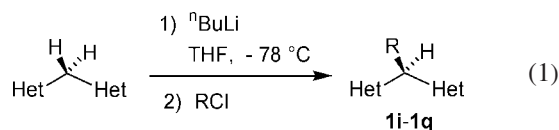
Department of Chemistry, The University of Chicago, 5735 South Ellis Avenue, Chicago, Illinois 60637

Received July 29, 2007

The catalytic ethylene polymerization reactions of $(N^{\wedge}N)PdMe(L)^+$ species that contain bulky bis(heterocycle)methane ligands were studied ($N^{\wedge}N = (1\text{-Me-imidazol-2-yl})_2CHCH(p\text{-tolyl})_2$ (**1i**), $(1\text{-Me-imidazol-2-yl})_2CHC(p\text{-tolyl})_3$ (**1j**), $(5\text{-Me-pyridin-2-yl})_2CHC(p\text{-tolyl})_2$ (**1k**), $(5\text{-Me-pyridin-2-yl})_2CHCH(p\text{-tolyl})_2$ (**1l**), $(3\text{-Me-pyridin-2-yl})_2CHCH(p\text{-tolyl})_2$ (**1m**), $(5\text{-Me-pyridin-2-yl})_2CHCH(m\text{-xylyl})_2$ (**1n**), $(3\text{-Me-pyridin-2-yl})_2CHCH(m\text{-xylyl})_2$ (**1o**), $(\text{quinol-2-yl})_2CHCH(m\text{-xylyl})_2$ (**1p**), and $(3\text{-Me-quinol-2-yl})_2CHCH(m\text{-xylyl})_2$ (**1q**)). $(N^{\wedge}N)PdMe_2$ (**2i,j,q**) and $(N^{\wedge}N)Pd(Me)Cl$ (**3m-o**) complexes were converted to $(N^{\wedge}N)Pd\{C(=O)Me\}CO^+$ complexes (**7i,j,m-o,q**). The ν_{CO} values for **7i,j,m-o,q** show that there is weak back-bonding in these species. Complexes **2i,j** and $(N^{\wedge}N)Pd(Me)Cl$ complexes **3l-o** were converted to $(N^{\wedge}N)Pd(Me)(H_2C=CH_2)^+$ (**8i,j,l-o** and **8q** (not directly observed)). First-order rate constants for ethylene insertion of **8i,j,l-o** were determined by NMR. Increasing the electrophilic character and the steric bulk of the $(N^{\wedge}N)Pd$ unit increases the rate of ethylene insertion. In-situ-generated **8j,l-n,q** produce low molecular weight polyethylene ($M_w \leq 4200$), while **8o** produces higher molecular weight polyethylene ($M_w = 34\,000$). Polyethylene produced by **8j,l,m** contains 100 branches/ 10^3 C, while that from **8n,o,q** contains 60 branches/ 10^3 C.

Introduction

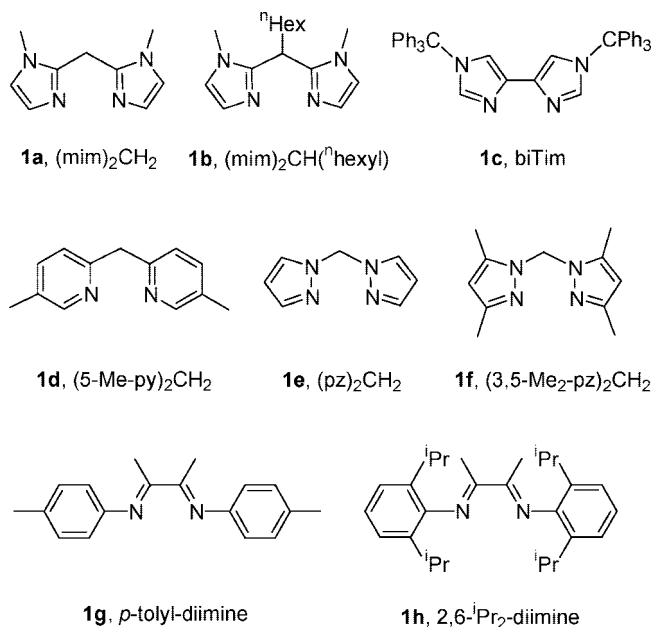
We recently described the reactivity of $(N^{\wedge}N)Pd(R)(\text{ethylene})^+$ species that contain the bis(heterocycle)methane ligands **1a-f**, which are shown in Chart 1.¹ These complexes catalytically dimerize ethylene by an insertion/ β -H elimination mechanism. The catalyst resting state was identified as the $(N^{\wedge}N)Pd(Et)(H_2C=CH_2)^+$ species. First-order rate constants ($k_{\text{insert,Me}}$) for ethylene insertion of $(N^{\wedge}N)Pd(Me)(\text{ethylene})^+$ species (**8a-f**) were determined by NMR. Ethylene insertion rates are enhanced as the electrophilic character and steric bulk of the $(N^{\wedge}N)Pd$ unit are increased. However, the most reactive $(N^{\wedge}N)Pd(Me)(\text{ethylene})^+$ species studied, **8f**, is ca. 3 and 12 times less reactive than analogous species **8g** and **8h**, which contain the α -diimine ligands **1g,h**.² In the present work, we have extended these studies to sterically bulky bis(heterocycle)methane ligands, in order to inhibit associative chain transfer and access ethylene polymerization catalysts,³ and to probe how steric effects influence the reactivity of $(N^{\wedge}N)Pd(R)(\text{ethylene})^+$ species.



Results and Discussion

$N^{\wedge}N$ Ligands. Ligands **1i-q** (Chart 2) were prepared by deprotonation of the parent (heterocycle)₂CH₂ compound followed

Chart 1



by quenching with the appropriate electrophile to install the capping substituent at the bridging methylene position (eq 1).⁴

$(N^{\wedge}N)PdX_2$ Complexes ($X = \text{Me}, \text{Cl}$). Synthetic routes to $(N^{\wedge}N)PdX_2$ complexes ($X = \text{Me}, \text{Cl}$) are shown in Scheme 1. The $(N^{\wedge}N)PdMe_2$ compounds **2i,j,q** were synthesized by ligand substitution of $[(\text{pyridazine})PdMe_2]_n$.⁵ Compounds **2i,j,q** are air- and water-stable but decompose slowly (days) in the solid state at 25 °C. The $(N^{\wedge}N)Pd(Me)Cl$ complexes **3l-o,q** were prepared by ligand substitution of $(\text{cod})Pd(Me)Cl$ ($\text{cod} = \text{cyclooctadiene}$).⁶ Compounds **3l-o,q** are more thermally stable than **2i,j,q**, but these species decompose slowly (weeks) at 25 °C in the solid state. The $(N^{\wedge}N)PdCl_2$ complexes **4i,m-q** were prepared

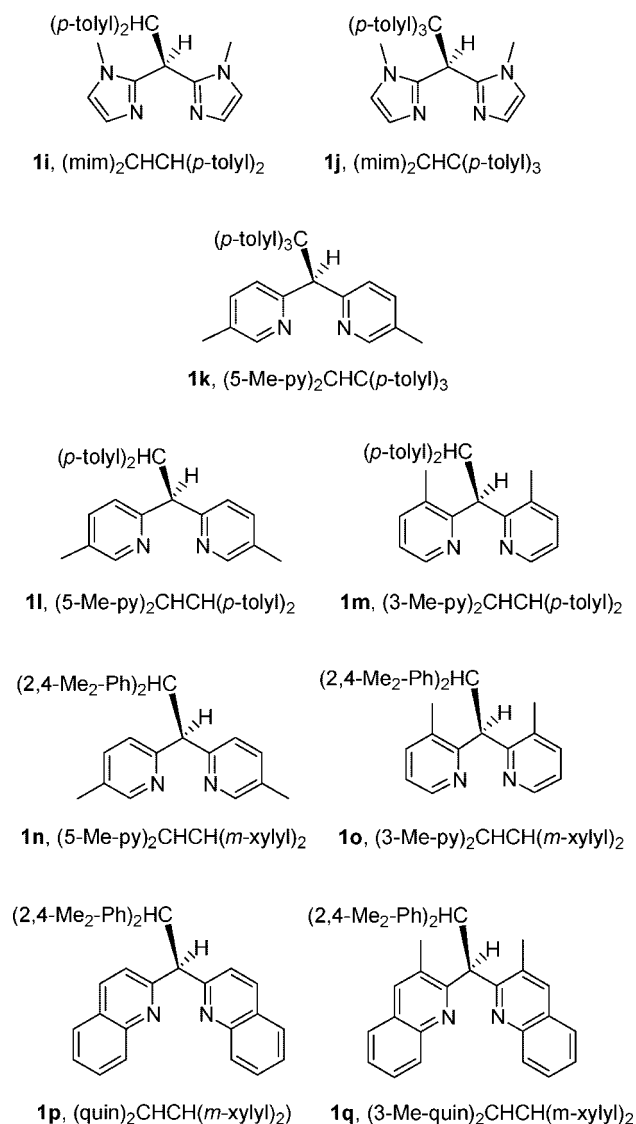
* Corresponding author. E-mail: rfjordan@uchicago.edu.

(1) Burns, C. T.; Jordan, T. F. *Organometallics* 2007, 26, 6726.

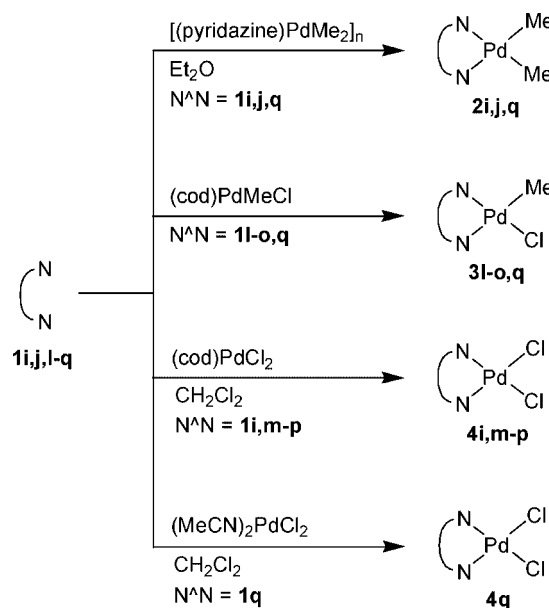
(2) Johnson, L. K.; Killian, C. M.; Brookhart, M. *J. Am. Chem. Soc.* 1995, 117, 6414.

(3) (a) Ittel, S. D.; Johnson, L. K.; Brookhart, M. *Chem. Rev.* 2000, 100, 1169. (b) Mecking, S. *Coord. Chem. Rev.* 2000, 203, 325.

Chart 2



Scheme 1



Molecular Structures of 4i,n,o,q. The structures of the dichloride complexes **4i,n,o,q** were determined by X-ray diffraction and are shown in Figures 1–4. These structures are similar to those of other {bis(heterocycle)methane}Pd^{II} complexes.^{7–13} In all four complexes, the geometry at Pd is square planar, the (N[^]N)Pd ring has a boat conformation, and the –CHAR₂ substituent on the bridging methylene carbon is in the axial position. The degree of (N[^]N)Pd ring boating can be assessed by the angles between the N–C–N and N–Pd–N planes, the N–C–C–N and C–C_{br}–C planes, and the two heterocycle ring planes. As the boating becomes more pronounced, these dihedral angles all decrease. These data are listed in Table 1 and show that the boating increases in the order **4i** < **4n,o** < **4q**.

Solution Structures of (N[^]N)Pd Complexes. The NMR spectra of **4i** contain one set of imidazole and *p*-tolyl resonances, indicative of a C_s-symmetric structure. The ¹H–¹H NOESY spectrum contains cross-peaks between the imidazole N-Me (δ 3.26) and (mim)₂CH (δ 4.68) resonances, consistent with a boat conformation of the (N[^]N)Pd ring and an axial –CH(*p*-tolyl)₂ group, as observed in the solid state. The spectra of **2i,j** are similar, implying similar structures.

The NMR spectra of **2q**, **3m–o,q**, and **4m–o,q** show that these species exist as single conformers in CD₂Cl₂ solution. The NOESY spectra and J_{HH} data are consistent with placement of the –CHAR₂ groups in the axial position, an anti orientation of the (heterocycle)₂CH and the CHAR₂ hydrogens, and, for the

by ligand substitution reactions of (cod)PdCl₂ or (MeCN)₂PdCl₂. Compounds **4i,m–q** are stable at 25 °C. The reaction of **1k** with (cod)PdCl₂ in CD₂Cl₂ did not produce {(*p*-tolyl)₃CHC(5-Me-py)₂}PdCl₂ (**4k**). After 24 h at 25 °C, the (cod)PdCl₂ and **1k** were completely consumed, but the only product that could be identified was free cod. It is likely that target **4k** is unstable due to extreme steric crowding between the –CAR₃ and (py)₂PdCl₂ units.

(4) (N[^]N) = (1-Me-imidazol-2-yl)₂CH₂ (**1a**, (mim)₂CH₂), (1-Me-imidazol-2-yl)₂CH(C₆H₁₃) (**1b**, (mim)₂CH(*n*-hexyl)), 1,1'-di(triphenylmethyl)-4,4'-biimidazole (**1c**, biTim), (5-Me-pyridin-2-yl)₂CH₂ (**1d**, (5-Mepy)₂CH₂), (pyrazol-1-yl)₂CH₂ (**1e**, (pz)₂CH₂), (3,5-Me₂-pyrazol-1-yl)₂CH₂ (**1f**, (3,5-Me₂-pz)₂CH₂), (4-Me-C₆H₄)N=CMeCMe=N(4-Me-C₆H₄) (**1g**, *p*-tolyl-diimine), and (2,6-ⁱPr₂-C₆H₃)N=CMeCMe=N(2,6-ⁱPr₂-C₆H₃) (**1h**, 2,6-ⁱPr₂-diimine), (1-Me-imidazol-2-yl)₂CH(CH(4-MeC₆H₄)₂) (**1i**, (mim)₂CH(CH(*p*-tolyl)₂)), (1-Me-imidazol-2-yl)₂CH(C(4-MeC₆H₄)₃) (**1j**, (mim)₂CH(C(*p*-tolyl)₃)), (5-Me-pyridin-2-yl)₂CH(C(4-MeC₆H₄)₃) (**1k**, (5-Me-py)₂CH(C(*p*-tolyl)₃)), (5-Me-pyridin-2-yl)₂CH(CH(4-MeC₆H₄)₂) (**1l**, (5-Me-py)₂CH(CH(*p*-tolyl)₂)), (3-Me-pyridin-2-yl)₂CH(CH(4-MeC₆H₄)₂) (**1m**, (3-Me-py)₂CH(CH(*p*-tolyl)₂)), (5-Me-pyridin-2-yl)₂CH(CH(2,4-Me₂-C₆H₃)₂) (**1n**, (5-Me-py)₂CH(CH(*m*-xylyl)₂)), (3-Me-pyridin-2-yl)₂CH(CH(2,4-Me₂-C₆H₃)₂) (**1o**, (3-Me-py)₂CH(CH(*m*-xylyl)₂)), (quinol-2-yl)₂CH(CH(2,4-Me₂-C₆H₃)₂) (**1p**, (quin)₂CH(CH(*m*-xylyl)₂)), and (3-Me-quinol-2-yl)₂CH(CH(2,4-Me₂-C₆H₃)₂) (**1q**, (3-Me-quin)₂CH(CH(*m*-xylyl)₂)).

(5) Byers, P. K.; Cauty, A. J. *Organometallics* **1990**, *9*, 210.

(6) Rülke, R. E.; Ernsting, J. M.; Spek, A. L.; Elsevier, C. J.; van Leeuwen, P. W. N. M.; Vrieze, K. *Inorg. Chem.* **1993**, *32*, 5769.

(7) Minghetti, G.; Cinellu, M. A.; Bandini, A. L.; Banditelli, G.; Demartin, F.; Manassero, M. *J. Organomet. Chem.* **1986**, *315*, 387.

(8) Burns, C. T.; Shen, H.; Jordan, R. F. *J. Organomet. Chem.* **2003**, *683*, 240.

(9) Tsuji, S.; Swenson, D. C.; Jordan, R. F. *Organometallics* **1999**, *18*, 4758.

(10) Done, M. C.; Ruther, T.; Cavell, K. J.; Kilner, M.; Peacock, E. J.; Braussaund, N.; Skelton, B. W.; White, A. J. *Organomet. Chem.* **2000**, *607*, 78.

(11) Newkome, G. R.; Gupta, V. K.; Theriot, K. J.; Ewing, J. C.; Wicelinski, S. P.; Huie, W. R.; Fronczek, F. R.; Watkins, S. F. *Acta Crystallogr., Sect. C: Cryst. Struct. Commun.* **1984**, *C40*, 1352.

(12) (a) Cauty, A. J.; Minchin, N. J.; Skelton, B. W.; White, A. H. *Aust. J. Chem.* **1992**, *45*, 423. (b) Newkome, G. R.; Gupta, V. K.; Taylor, H. C. R.; Fronczek, F. R. *Organometallics* **1984**, *3*, 1549.

(13) Jalón, F. A.; Manzano, B. R.; Otero, A.; Rodríguez-Perez, M. C. *J. Organomet. Chem.* **1995**, *494*, 179.

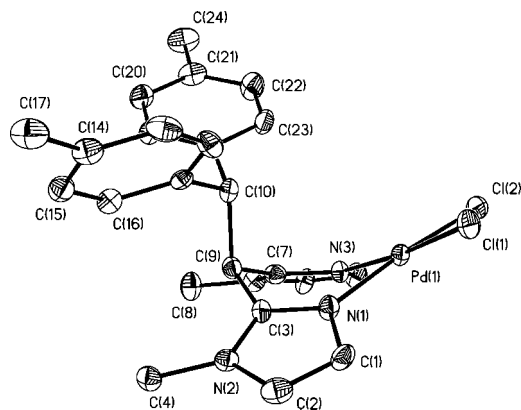


Figure 1. ORTEP view of $\{(p\text{-tolyl})_2\text{HCHC}(\text{mim})_2\}\text{PdCl}_2$ (**4i**). Thermal ellipsoids are drawn at 50% probability level. Hydrogen atoms are omitted. Key bond distances (Å) and angles (deg): Cl(1)–Pd(1) 2.28(2); N(1)–Pd(1) 2.02(4); Cl(2)–Pd(1) 2.29(2); N(3)–Pd(1) 2.02(4); C(9)–C(10) 1.56(5); N(1)–Pd(1)–N(3) 87.0(2); N(3)–Pd(1)–Cl(1) 174.2(1); N(3)–Pd(1)–Cl(2) 91.0(1); N(1)–Pd(1)–Cl(1) 91.4(2); N(1)–Pd(1)–Cl(2) 175.0(2); Cl(1)–Pd(1)–Cl(2) 91.1(6).

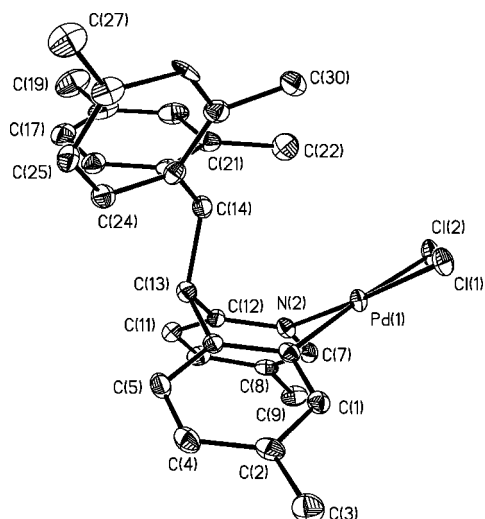


Figure 2. ORTEP view of $\{(m\text{-xylyl})_2\text{HCHC}(5\text{-Me-py})_2\}\text{PdCl}_2$ (**4n**). Thermal ellipsoids are drawn at 50% probability level. Hydrogen atoms are omitted. Key bond distances (Å) and angles (deg): Cl(1)–Pd(1) 2.29(8); N(1)–Pd(1) 2.02(2); Cl(2)–Pd(1) 2.29(8); N(2)–Pd(1) 2.04(2); C(13)–C(14) 1.56(6); N(1)–Pd(1)–N(2) 87.0(9); N(2)–Pd(1)–Cl(1) 176.6(7); N(2)–Pd(1)–Cl(2) 90.8(7); N(1)–Pd(1)–Cl(1) 91.3(7); N(1)–Pd(1)–Cl(2) 175.7(7); Cl(1)–Pd(1)–Cl(2) 91.1(3).

m-xylyl cases, orientation of the *m*-xylyl rings such that the 2-Me groups point toward Pd. These results are consistent with the solid state structures of **4n**, **o**, **q**. For example, the NOESY spectrum of **3o** contains cross-peaks between the (3-Me-py)₂CH (δ 5.45) and (3-Me-py)₂CH (δ 2.57) resonances and between one of the *m*-xylyl 2-Me resonances (δ 2.35) and the PdMe resonance (δ 0.66), but not between the (3-Me-py)₂CH and CH(*m*-xylyl)₂ resonances. The (3-Me-py)₂CH/CH(*m*-xylyl)₂ ³J_{HH} value is 11 Hz.

In contrast, the NMR spectra of **4p** show that this species exists as an 86/14 mixture of two conformers in CD₂Cl₂ solution at 25 °C. In the major isomer (**4p**-H_{eq}), the (quin)₂CH hydrogen is equatorial and the –CHAr₂ group is axial, and in the minor isomer (**4p**-H_{ax}) these positions are reversed, as shown in Figure 5. The NOESY spectrum contains a cross-peak between the (quin)₂CH resonance (δ 5.76) and the quinoline H3 resonance

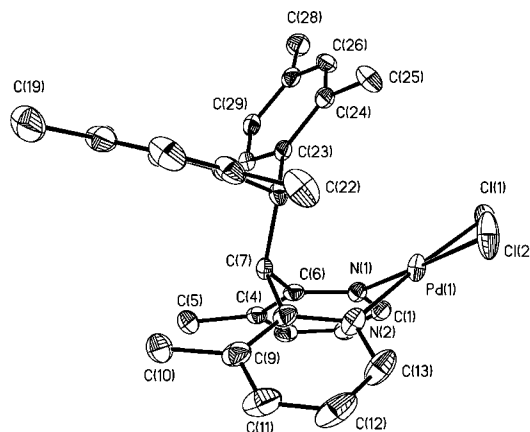


Figure 3. ORTEP view of $\{(m\text{-xylyl})_2\text{HCHC}(3\text{-Me-py})_2\}\text{PdCl}_2$ (**4o**). Thermal ellipsoids are drawn at 50% probability level. Hydrogen atoms are omitted. Key bond distances (Å) and angles (deg): Cl(1)–Pd(1) 2.30(7); N(2)–Pd(1) 2.04(2); Cl(2)–Pd(1) 2.30(8); N(1)–Pd(1) 2.03(2); C(7)–C(14) 1.57(9); N(2)–Pd(1)–N(1) 87.0(8); N(1)–Pd(1)–Cl(2) 177.8(5); N(1)–Pd(1)–Cl(1) 92.6(6); N(2)–Pd(1)–Cl(2) 91.6(6); N(2)–Pd(1)–Cl(1) 176.5(6); Cl(2)–Pd(1)–Cl(1) 88.9(3).

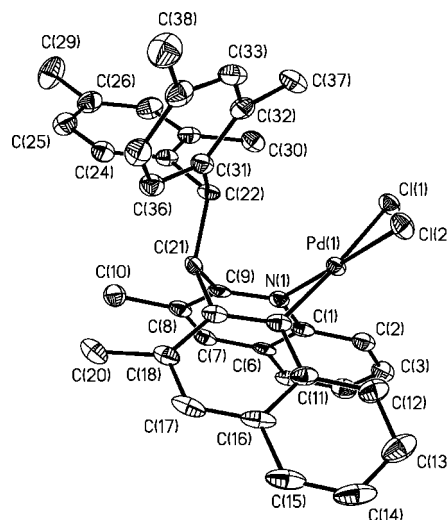


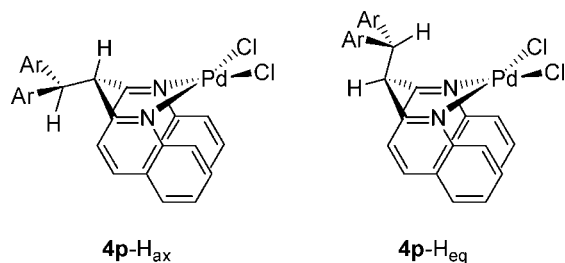
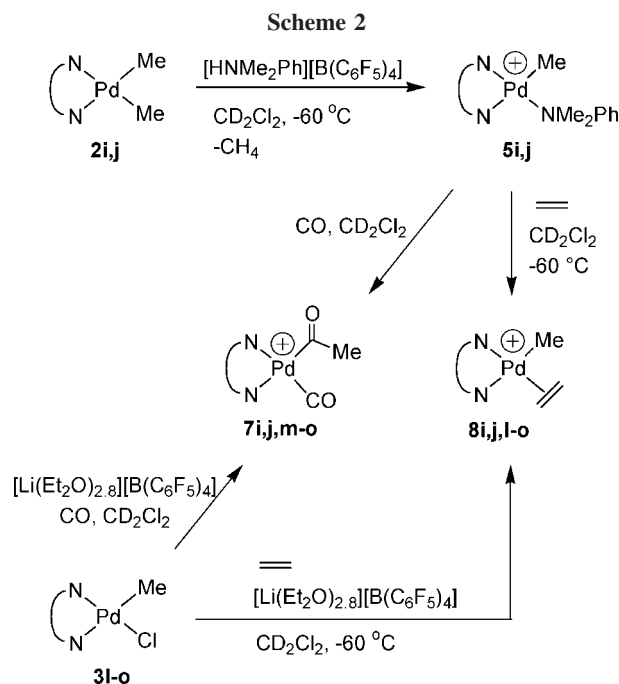
Figure 4. ORTEP view of $\{(m\text{-xylyl})_2\text{HCHC}(3\text{-Me-quin})_2\}\text{PdCl}_2$ (**4q**). Thermal ellipsoids are drawn at 50% probability level. Hydrogen atoms are omitted. Key bond distances (Å) and angles (deg): Cl(1)–Pd(1) 2.30(1); Cl(2)–Pd(1) 2.29(1); N(2)–Pd(1) 2.03(4); N(1)–Pd(1) 2.05(4); C(21)–C(22) 1.57(8); N(2)–Pd(1)–N(1) 83.0(2); N(1)–Pd(1)–Cl(2) 177.4(1); N(1)–Pd(1)–Cl(1) 90.6(2); N(2)–Pd(1)–Cl(2) 94.9(1); N(2)–Pd(1)–Cl(1) 175.5(1); Cl(2)–Pd(1)–Cl(1) 93.7(1).

Table 1. Dihedral angles between planes (deg) for (N[^]N)PdCl₂ Complexes

dihedral angle	4i	4n	4o	4q
N–C–N/N–Pd–N	154.83	144.48	144.85	134.07
N–C–N/N–C–C _{br} –C	141.65	132.52	127.4	129.39
het-1/het-2	133.57	118.70	116.85	100.70

for **4p**-H_{eq}. The CH(*m*-xylyl)₂ resonance of **4p**-H_{eq} appears at low field (δ 8.52) due to the proximity of this hydrogen to Pd. For **4p**-H_{ax}, the (quin)₂CH resonance is shifted downfield (δ 9.14) due to the proximity of this hydrogen to Pd, and the CH(*m*-xylyl)₂ resonance is shifted upfield (δ 5.72) due to anisotropic shielding by the quinoline rings.

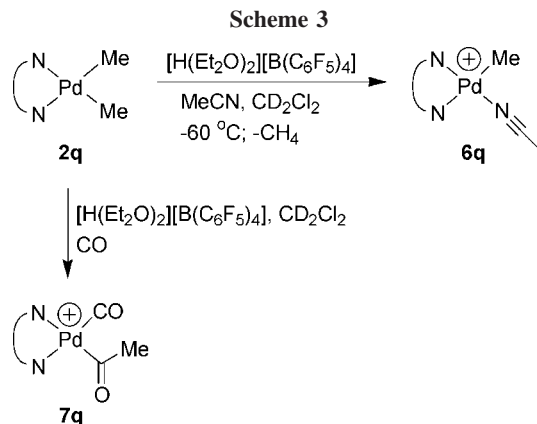
Complex **3l** exists as a single conformer at room temperature, which exhibits similar NMR spectra to those of **3n** and is

Figure 5. The two conformers of **4p**.

therefore assigned as **3i-H_{eq}**, in which the $-\text{CH}(p\text{-tolyl})_2$ group is axial. However at low temperature, **3i** exists a mixture of **3i-H_{eq}** and **3i-H_{ax}** conformers. The isomer ratio **3i-H_{eq}**/**3i-H_{ax}** is ca. 1/2 at $-60\text{ }^\circ\text{C}$. **3i-H_{ax}** may be favored at low temperature due to the loss of entropy from inhibition of rotation of the $-\text{CH}(p\text{-tolyl})_2$ group. Exchange of **3i-H_{eq}** and **3i-H_{ax}** is fast on the laboratory time scale but slow on the NMR time scale.

The *H_{eq}* conformers of $\{\text{RHC}(\text{heterocycle})_2\}\text{Pd}$ complexes are usually favored because steric crowding between the $(\text{heterocycle})_2\text{CHR}$ group and the heterocycle rings is less severe than in the *H_{ax}* conformers. However, as the boating of the $(\text{N}^{\wedge}\text{N})\text{Pd}$ ring becomes more pronounced, e.g., by moving from imidazole to pyridine-based ligands and incorporating substituents in the 6-positions of the pyridine rings, the $(\text{heterocycle})_2\text{CHR}$ group is forced close to the Pd center in the *H_{eq}* conformer. This effect favors formation of the *H_{ax}* conformers for **3i** and **4p**. In contrast, incorporating substituents at the 3-positions of the pyridine rings and increasing the size of the $(\text{pyridine})_2\text{CHR}$ group results in severe crowding between the $(\text{pyridine})_2\text{CHR}$ group and the pyridine rings in the *H_{ax}* conformer. This effect favors formation of the *H_{eq}* conformer for **3m-o,q** and **4m-o,q**.

Generation of $(\text{N}^{\wedge}\text{N})\text{PdMe}(\text{NMe}_2\text{Ph})^+$ Species (5i,j**).** The reaction of **2i,j** with $[\text{HNMe}_2\text{Ph}][\text{B}(\text{C}_6\text{F}_5)_4]$ in CD_2Cl_2 at $-60\text{ }^\circ\text{C}$ generates $[(\text{N}^{\wedge}\text{N})\text{PdMe}(\text{NMe}_2\text{Ph})][\text{B}(\text{C}_6\text{F}_5)_4]$ (**5i,j**, Scheme 2) cleanly. Complexes **5i,j** are stable at low temperature ($-60\text{ }^\circ\text{C}$) but decompose slowly at $25\text{ }^\circ\text{C}$ to yield black solutions and NMe_2Ph ; the fate of the $(\text{N}^{\wedge}\text{N})\text{PdMe}^+$ unit was not determined. The $-60\text{ }^\circ\text{C}$ ^1H NMR spectra of **5i,j** show that the

Table 2. Pd-CO ^{13}C NMR Chemical Shifts (δ) and ν_{CO} Values of $(\text{N}^{\wedge}\text{N})\text{Pd}\{\text{C}(\text{=O})\text{Me}\}\text{CO}^+$ Complexes in CD_2Cl_2 Solution

complex	$\text{N}^{\wedge}\text{N}$ ligand	δ ^{13}C Pd-CO	ν_{CO} (cm^{-1})
7i	$(\text{mim})_2\text{CH}(\text{CH}(p\text{-tolyl})_2)$	173.5 ^b	2123 ^a
7j	$(\text{mim})_2\text{CH}(\text{C}(p\text{-tolyl})_3)$	172.7 ^b	2118 ^a
7m	$(3\text{-Me-py})_2\text{CH}(\text{CH}(p\text{-tolyl})_2)$	172.8 ^b	2127 ^a
7n	$(5\text{-Me-py})_2\text{CH}(\text{CH}(m\text{-xylyl})_2)$	172.7 ^c	2127 ^a
7o	$(3\text{-Me-py})_2\text{CH}(\text{CH}(m\text{-xylyl})_2)$	172.5 ^c	2127 ^a
7q	$(3\text{-Me-quin})_2\text{CH}(\text{CH}(m\text{-xylyl})_2)$	172.7 ^b	2126 ^a

^a $23\text{ }^\circ\text{C}$. ^b $-40\text{ }^\circ\text{C}$. ^c $-60\text{ }^\circ\text{C}$.

sides of the $\text{N}^{\wedge}\text{N}$ ligands are inequivalent and one NMe_2Ph ligand is present. In both cases, one mim-H4 resonance appears at a high field (δ 4.69 for **5i**; δ 5.23 for **5j**) due to anisotropic shielding by the NMe_2Ph ring.

Generation of $\{(m\text{-xylyl})_2\text{HCCH}(3\text{-Me-quin})_2\}\text{PdMe}(\text{NCMe})[\text{B}(\text{C}_6\text{F}_5)_4]$ (6q**).** The reaction of **2q** with $[\text{H}(\text{OEt}_2)_2][\text{B}(\text{C}_6\text{F}_5)_4]$ in CD_2Cl_2 at $-60\text{ }^\circ\text{C}$ proceeds with the consumption of the reactants and produces a colorless solution. The anticipated $(\text{N}^{\wedge}\text{N})\text{PdMe}(\text{OEt}_2)^+$ product could not be identified. However, addition of acetonitrile to this solution yields $\{(m\text{-xylyl})_2\text{HCCH}(3\text{-Me-quin})_2\}\text{PdMe}(\text{NCMe})[\text{B}(\text{C}_6\text{F}_5)_4]$ (**6q**), as shown in Scheme 3. The $-60\text{ }^\circ\text{C}$ ^1H NMR spectrum of **6q** shows that the sides of the $(3\text{-Me-quin})_2\text{CHCH}(m\text{-xylyl})_2$ ligand are inequivalent and one acetonitrile ligand is present. The chemical shift for the bound acetonitrile (δ 2.29) is similar to that for $(2,2'\text{-bipyridine})\text{PdMe}(\text{NCMe})^+$.¹⁴

Generation of $(\text{N}^{\wedge}\text{N})\text{Pd}\{\text{C}(\text{=O})\text{Me}\}\text{CO}^+$ Species (7i,j,m-o,q**).** The acyl carbonyl complexes $[(\text{N}^{\wedge}\text{N})\text{Pd}\{\text{C}(\text{=O})\text{Me}\}\text{CO}][\text{B}(\text{C}_6\text{F}_5)_4]$ (**7i,j,m-o,q**) were prepared as shown in Schemes 2 and 3. Exposure of frozen CD_2Cl_2 solutions of **5i,j** to CO followed by brief warming to $25\text{ }^\circ\text{C}$ yields **7i,j**. The reaction of **3m-o** with $[\text{Li}(\text{Et}_2\text{O})_{2.8}][\text{B}(\text{C}_6\text{F}_5)_4]$ in CD_2Cl_2 in the presence of CO at $25\text{ }^\circ\text{C}$ yields **7m-o**. Exposure of a frozen CD_2Cl_2 solution containing the product of the reaction of **2q** and $[\text{H}(\text{OEt}_2)_2][\text{B}(\text{C}_6\text{F}_5)_4]$ to CO, followed by brief warming to $25\text{ }^\circ\text{C}$, yields **7q** (Scheme 3). Complexes **7i,j,m-o,q** are stable at low temperature (-78 to $-40\text{ }^\circ\text{C}$) but decompose within several hours at $25\text{ }^\circ\text{C}$.

Complexes **7i,j,m-o,q** were characterized by NMR at $-40\text{ }^\circ\text{C}$ (**7i,j,m,q**) or $-60\text{ }^\circ\text{C}$ (**7n,o**) in CD_2Cl_2 in the presence of excess CO. The Pd-CO ^{13}C NMR chemical shifts fall within a narrow range (δ 171.3 to 173.5; Table 2) and are shifted upfield from the free CO resonance (δ 184.0). The Pd-CO and free CO ^{13}C resonances are sharp, indicating that CO exchange is slow on the NMR time scale under these conditions.

The PdCO ν_{CO} values for **7i,j,m-o,q** are listed in Table 2. These species exhibit high ν_{CO} values (cf. $\nu_{\text{CO}} = 2139\text{ cm}^{-1}$

(14) Brookhart, M.; Rix, F. C.; DeSimone, J. M.; Barborak, J. C. *J. Am. Chem. Soc.* **1992**, *114*, 5894.

Table 3. First-Order Rate Constants ($k_{\text{insert,Me}}$) for Ethylene Insertion of $(N^{\wedge}N)\text{PdMe}(\text{H}_2\text{C}=\text{CH}_2)^+$ in CD_2Cl_2 at -10°C

compound	$N^{\wedge}N$ ligand	$k_{\text{insert,Me}}$ (10^{-4} s^{-1})
8i	(mim) ₂ CH(CH(<i>p</i> -tolyl) ₂)	1.6(1)
8j	(mim) ₂ CH(C(<i>p</i> -tolyl) ₃)	3.0(1)
8l	(5-Me-py) ₂ CH(CH(<i>p</i> -tolyl) ₂)	10.1(1) ^a
8m	(3-Me-py) ₂ CH(CH(<i>p</i> -tolyl) ₂)	5.0(5)
8n	(5-Me-py) ₂ CH(CH(<i>m</i> -xylyl) ₂)	10.1(1)
8o	(3-Me-py) ₂ CH(CH(<i>m</i> -xylyl) ₂)	13(1)

^aRate constant for reaction of the total of the **8i**-H_{eq} and **8i**-H_{ax} conformers.

for free CO in CD_2Cl_2) characteristic of electrophilic metal centers.¹⁵ The ν_{CO} values vary in the order **7i,j** < **7m-o,q**, consistent with the stronger donor ability of imidazole versus pyridine ligands. These data, and results for analogous complexes based on ligands **1a,b,d**,¹ show that variation of the capping substituent or the pyridine ring substituents does not strongly affect the donor property of the bis(heterocycle)methane ligand.

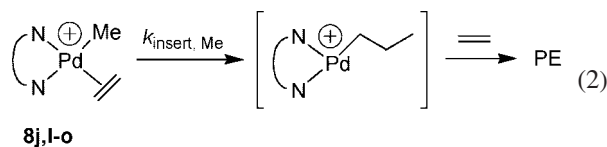
Generation of $(N^{\wedge}N)\text{PdMe}(\text{H}_2\text{C}=\text{CH}_2)[\text{B}(\text{C}_6\text{F}_5)_4]$ Species (8i,j,l-o**).** The methyl ethylene complexes $[(N^{\wedge}N)\text{PdMe}(\text{H}_2\text{C}=\text{CH}_2)][\text{B}(\text{C}_6\text{F}_5)_4]$ (**8i,j,l-o**) were generated as shown in Scheme 3. The reaction of **5i,j** with ethylene at -60°C yields **8i,j** by displacement of the NMe_2Ph ligand.¹⁶ The reaction of **3l-o** with $[\text{Li}(\text{Et}_2\text{O})_{2,8}][\text{B}(\text{C}_6\text{F}_5)_4]$ in the presence of ethylene yields **8l-o**. Complex **8l** exists as a 2/3 **8l**-H_{eq}/**8l**-H_{ax} mixture at -40°C . Complexes **8i,j,l-o** are stable in CD_2Cl_2 solution at -60°C , but undergo insertion at higher temperatures (ca. -40°C (**8o**) to -20°C (**8i,j**)). The free NMe_2Ph (**8i,j**) or Et_2O (**8l-o**) released in the generation of these species has no effect on subsequent chemistry, but can be used as an internal standard for NMR integration.

Attempts to observe $\{(m\text{-xylyl})_2\text{HCHC}(3\text{-Me-quin})_2\}\text{-PdMe}(\text{H}_2\text{C}=\text{CH}_2)^+$ (**8q**) were unsuccessful. This species was not detected in the reactions of **2q** and $[\text{H}(\text{OEt})_2][\text{B}(\text{C}_6\text{F}_5)_4]$, or **3q** and $\text{Ti}[\text{B}(\text{C}_6\text{F}_5)_4]$, in the presence of ethylene from -60 to 0°C , and ethylene does not displace acetonitrile from **6q** at low temperature. Steric crowding may inhibit ethylene binding to the $\{(m\text{-xylyl})_2\text{HCHC}(3\text{-Me-quin})_2\}\text{PdMe}^+$ cation.

The ^1H NMR spectra of **8i,j,l-o** in the presence of excess ethylene at -60°C (**8i,m-o**) and -40°C (**8j,l**) contain separate signals for bound and free ethylene, indicating that intermolecular exchange of ethylene is slow. This contrasts with the fast exchange observed for analogous species **8a,d**, which lack a capping substituent. The $-\text{CHAr}_2$ groups and the boating of the $(N^{\wedge}N)\text{Pd}$ chelate rings hinder access to the axial coordination sites and inhibit associative ligand exchange processes. Slow ethylene exchange was also observed for **8b**, which contains an axial *n*-hexyl substituent.¹

Ethylene Insertion of $(N^{\wedge}N)\text{PdMe}(\text{H}_2\text{C}=\text{CH}_2)^+$ Species. Complexes **8i,j,l-o** undergo ethylene insertion, which, in the presence of excess ethylene, leads to branched polyethylene (PE) formation as shown in eq 2. The rate of ethylene insertion of **8i,j,l-o** was measured by ^1H NMR monitoring of the disappearance of the Pd–Me resonance at -10°C . The first-order rate constants for insertion ($k_{\text{insert,Me}}$) are listed in Table 3.

Ethylene Polymerization by **8j,l-o,q.** Cationic $(N^{\wedge}N)\text{PdMe}^+$ species polymerize ethylene to low molecular weight, highly



branched polyethylene (eq 2). Polymerizations were performed by generating $(N^{\wedge}N)\text{Pd}(\text{Me})(\text{ethylene})^+$ species in CH_2Cl_2 or $\text{C}_6\text{H}_5\text{Cl}$ in the presence of ethylene by the reaction of $(N^{\wedge}N)\text{PdMe}_2$ complexes **2** with $[\text{HNMe}_2\text{Ph}][\text{B}(\text{C}_6\text{F}_5)_4]$ or by reaction of $(N^{\wedge}N)\text{PdMeCl}$ complexes **3** with $[\text{Li}(\text{Et}_2\text{O})_{2,8}][\text{B}(\text{C}_6\text{F}_5)_4]$ or $\text{Ti}[\text{B}(\text{C}_6\text{F}_5)_4]$ (cf. Scheme 2).¹⁷ In the case of ligand **q**, the $(N^{\wedge}N)\text{Pd}(\text{Me})(\text{ethylene})^+$ complex **8q** was not directly observed but is assumed to form in the first step of the polymerization. Representative results are given in Table 4.

The polymer yields vary in the order **8o** > **8m** > **8j,l,n** > **8q**. With the exception of **8o**, these catalysts produce very low molecular weight polyethylene ($M_w = 1300\text{--}4200$; $X_n =$ number average degree of polymerization = 24–69). However, **8o** produces polyethylene with $M_w = 23\,000$ in CH_2Cl_2 and 36 000 in $\text{C}_6\text{H}_5\text{Cl}$ solvent.¹⁸ The polyethylenes from **8j,l,m** contain ca. 100 branches/ 10^3 carbons, similar to what is observed for other palladium catalysts.³ In contrast, polymers from **8n,o,q** contain only 53–66 branches/ 10^3 carbons. These differences are reflected in the physical properties of the polyethylenes. The polymers produced by **8j,l,m** are oils, those from **8n,q** are waxes, and those from **8o** are solids.

Assessment of Steric Properties by the Accessible Molecular Surface Model. The accessible molecular surface (AMS) model developed by Angermund et al. was used to assess the steric properties of the $(N^{\wedge}N)\text{PdR}^+$ catalysts.¹⁹ The AMS model approximates the surface area of the metal in a complex that is accessible to a probe molecule. Molecular surfaces for $(N^{\wedge}N)\text{Pd}(\text{II})$ units were generated using the molecular surface generator developed by Connolly.²⁰ A probe of radius 1.4 Å (ca. the radius of a water molecule) was rolled over the surface, and the accessible surface at Pd (AMS) was determined. The results are listed in Table 5. The results for static $(N^{\wedge}N)\text{Pd}$ units based on X-ray crystallographic results for $(N^{\wedge}N)\text{Pd}$ complexes,²¹ and models of $(N^{\wedge}N)\text{PdCl}_2$ complexes generated by molecular mechanics,²² are similar. Smaller AMS values correspond to more crowded complexes.

Influence of Electronic and Steric Properties of $(N^{\wedge}N)\text{PdMe}(\text{H}_2\text{C}=\text{CH}_2)^+$ Species on Reactivity. The rate constants for ethylene insertion of $(N^{\wedge}N)\text{PdMe}(\text{H}_2\text{C}=\text{CH}_2)^+$ species ($k_{\text{insert,Me}}$) provide a measure of the inherent insertion

(17) Schmid, M.; Eberhardt, R.; Klinga, M.; Leskelä, M.; Rieger, B. *Organometallics* **2001**, *20*, 2321.

(18) (a) Similarly, for (α -diimine)Pd catalysts, polyethylene molecular weights typically double when the polymerization solvent is changed from CH_2Cl_2 to $\text{C}_6\text{H}_5\text{Cl}$. See: Gottfried, A. C.; Brookhart, M. *Macromolecules* **2003**, *36*, 3085. (b) Gottfried, A. C.; Brookhart, M. *Macromolecules* **2001**, *34*, 1140.

(19) (a) Angermund, K.; Baumann, W.; Dinjus, E.; Fornika, R.; Goerls, H.; Kessler, M.; Krueger, C.; Leitner, W.; Lutz, F. *Chem.–Eur. J.* **1997**, *3*, 755. (b) Reetz, M. T.; Haderlein, G.; Angermund, K. *J. Am. Chem. Soc.* **2000**, *122*, 996. (c) Haenel, M. W.; Oevers, S.; Angermund, K.; Kaska, W. C.; Fan, H.-J.; Hall, M. B. *Angew. Chem.* **2001**, *40*, 3596.

(20) (a) Connolly, M. L. *Science* **1983**, *221*, 709. (b) Connolly, M. L. *J. Appl. Crystallogr.* **1983**, *16*, 548.

(21) (a) For **1d**, $\text{H}_2\text{C}(\text{py})_2\text{Pd}(\text{OR})_2$ ($\text{R} = \text{C}_5\text{H}_7\text{N}_2\text{O}$): Mock, C.; Puscasu, I.; Rauterkus, M. J.; Geshe, T.; Wolff, J. E. A.; Krebs, B. *Inorg. Chim. Acta* **2001**, *319*, 109. (b) For **1e**, $\text{H}_2\text{C}(\text{pz})_2\text{Pd}(\text{S}_2\text{CNC}_5\text{H}_{10})$: Sánchez, G.; Serrano, J. L.; Ramirez de Arellano, M. C.; Pérez, J.; Lopez, G. *Polyhedron* **2000**, *19*, 1395. (c) For **1f**, $\text{H}_2\text{C}(3,5\text{-Me}_2\text{-pz})_2\text{Pd}(\text{salicylaldehyde})$: Sánchez, G.; Serrano, J. L.; Pérez, J.; Ramirez de Arellano, M. C.; Lopez, G.; Molins, E. *Inorg. Chim. Acta* **1999**, *295*, 136. (d) For **1i,n,o,q**, complexes **4i,n,o,q**; this work.

(22) MMFF. Titan, version 1.0.5; Wavefunction, Inc.: San Diego, 2000.

(15) (a) Rix, F. C.; Brookhart, M.; White, P. S. *J. Am. Chem. Soc.* **1996**, *118*, 4746. (b) Guo, Z.; Swenson, D. C.; Guram, A. S.; Jordan, R. F. *Organometallics* **1994**, *13*, 766. (c) Foley, S. R.; Shen, H.; Qadeer, U. A.; Jordan, R. F. *Organometallics* **2004**, *23*, 600.

(16) Wu, F.; Foley, S. R.; Burns, C. T.; Jordan, R. F. *J. Am. Chem. Soc.* **2005**, *127*, 1841.

Table 4. Ethylene Polymerization Data^a

entry	catalyst	solvent	yield (g)	TON ^b	B ^c	M _w ^d	M _w /M _n ^e	X _n ^f
1	8j ^g	CH ₂ Cl ₂	0.83	988	101	1844	1.68	39
2	8l ^h	CH ₂ Cl ₂	1.10	1310	98	2026	2.33	31
3	8m ^h	CH ₂ Cl ₂	1.56	1860	96	4159	2.14	69
4	8o ^h	CH ₂ Cl ₂	2.29	2730	63	23406	1.89	442
5	8n ^h	C ₆ H ₅ Cl	0.94	1083	64	3461	2.22	56
6	8o ^h	C ₆ H ₅ Cl	2.25	2679	53	34585	1.88	657
7	8q ⁱ	C ₆ H ₅ Cl	0.32	381	66	1293	1.85	25

^a Polymerization conditions: 3.0 atm ethylene, 25 °C, 18 h, 30.0 μmol catalyst, 20 mL solvent. ^b Turnover number (moles of ethylene polymerized per mole of catalyst). ^c Branches per 10³ carbons determined by ¹H NMR. ^d Weight average molecular weight determined by GPC. ^e Polydispersity determined by GPC. ^f Number average degree of polymerization. ^g Generated in situ from **2** and [HNMe₂Ph][B(C₆F₅)₄]. ^h Generated in situ from **3** and [Li(Et₂O)₂][B(C₆F₅)₄]. ⁱ Generated in situ from **3** and Ti[B(C₆F₅)₄]; not observed.

Table 5. Calculated Pd Accessible Molecular Surface (AMS) Values for (N[^]N)Pd^{II} Units

N [^] N ligand	AMS _{X-ray} (Å ²) ^a	AMS _{MM} (Å ²) ^b
1a , (mim) ₂ CH ₂		9.86
1d , (5-Me-py) ₂ CH ₂	8.33	8.13
1e , (pz) ₂ CH ₂	10.88	9.69
1f , (3,5-Me ₂ -pz) ₂ CH ₂	6.12	6.53
1g , <i>p</i> -tolylidimine		9.72
1i , (mim) ₂ CH(CH(<i>p</i> -tolyl) ₂)	7.72	7.31
1j , (mim) ₂ CH(C(<i>p</i> -tolyl) ₃)		5.17
1m , (3-Me-py) ₂ CH(CH(<i>p</i> -tolyl) ₂)		5.17
1n , (5-Me-py) ₂ CH(CH(<i>m</i> -xylyl) ₂)	3.67	4.05
1o , (3-Me-py) ₂ CH(CH(<i>m</i> -xylyl) ₂)	3.37	3.77
1q , (3-Me-quin) ₂ CH(CH(<i>m</i> -xylyl) ₂)	1.12	1.09

^a Based on X-ray structural data for (N[^]N)Pd(II) compounds. ^b Based on models of (N[^]N)PdCl₂ complexes generated by molecular mechanics.

reactivity of (N[^]N)PdR(H₂C=CH₂)⁺ catalysts. The dependence of *k*_{insert,Me} for ethylene dimerization catalysts **8a,d-f**, and ethylene polymerization catalysts **8i,j,m-o**, on the ν_{CO} value for the corresponding (N[^]N)Pd{C(=O)Me}(CO)⁺ species and the AMS value for the (N[^]N)Pd unit is shown in Figure 6. In general, higher ν_{CO} values (more electron-deficient Pd centers) and lower AMS values (more crowded Pd centers) result in faster ethylene insertion rates. Complexes that contain weak donor pyridine and pyrazole ligands (**8d-f,m-o**) have higher *k*_{insert,Me} values than sterically similar complexes that contain stronger donor imidazole ligands (**8a,i,j**). Large substituents on the N[^]N ligand increase the rate of ethylene insertion (**8j** vs **8a**; **8f** vs **8e**; **8o** vs **8m**). A more electron-deficient Pd center provides less d-π* back-bonding and may generate greater δ⁺ character on the bound ethylene, which lowers the insertion barrier. Steric crowding promotes insertion by providing steric driving force to decrease the coordination number. However, ethylene polymerization activities of (N[^]N)PdR(H₂C=CH₂)⁺ catalysts do not directly parallel trends in *k*_{insert,Me} values, since factors such as catalyst activation efficiency, β-agostic interactions in higher alkyls, steric inhibition to ethylene coordination, and catalyst deactivation may differ between the catalysts.

While Figure 6 provides useful insights into the reactivity trends for (N[^]N)PdMe(H₂C=CH₂)⁺ species, it is clear that the AMS values are insufficient to understand the steric effects among catalysts that have very different structures, since the specific arrangement of bulky groups is critical. A case in point is the comparison of ligands **1e** and **1g**. The (**1g**)Pd and (**1e**)Pd units have very similar AMS values, and the corresponding (N[^]N)Pd{C(=O)Me}CO⁺ complexes (**7e,g**) have very similar ν_{CO} values. However, *k*_{insert,Me} for **8g** is ca. 10 times higher than that for **8e**.¹ The imine N-aryl rings in **8g** provide steric pressure in the correct location to enhance the ethylene insertion rate (Figure 7).

The sterically open complexes **8a** and **8d** dimerize ethylene, as noted above. Incorporation of -CHAr₂ or CAR₃ substituents in the bridging methylene linker of the (N[^]N) ligands in the analogues **8j** and **8l,n** shifts the product distribution to higher molecular weights. As the ethylene insertion rates of **8a** and **8j**, and of **8d** and **8l,n**, are similar, this increase must result from a reduction in the chain transfer rate.²³ As noted above in the discussion of ethylene exchange rates, the bulky groups inhibit access to the axial coordination sites and therefore inhibit associative chain transfer processes. This trend has been observed in other Pd catalysts.^{2,3a,17,24}

Interestingly, **8o**, which contains a -CH(*m*-xylyl)₂ capping group, produces much higher molecular weight polyethylene than analogue **8m**, which contains a -CH(*p*-tolyl)₂ group. As *k*_{insert,Me} for **8o** is only 2.6 times greater than that for **8m**, this difference also likely results from a difference in chain transfer rate. The two 2-Me groups of the *m*-xylyl unit sit directly above the Pd in (N[^]N)PdCl₂ complex **4o** (X-ray and NOESY) and (N[^]N)Pd(Me)Cl complex **3o** (NOESY). A similar arrangement is expected for active (N[^]N)PdR(ethylene)⁺ species. These methyl groups effectively block the axial face of the Pd and inhibit associative chain transfer. Catalyst **8o**, which contains 3-Me-py substituents, also produces much higher molecular weight polyethylene than analogue **8n**, which contains 5-Me-py substituents. The 3-Me-py substituents induce slightly more boating in the (N[^]N)Pd chelate ring (see Table 1), which increases steric hindrance at the axial sites. Additionally, the 3-Me-py substituents may decrease the flexibility of the (N[^]N)Pd chelate ring (cf. conformer distribution of **3m** vs **3l** and **4q** vs **4p**), which could hinder associative chain transfer processes.

The -CH(*m*-xylyl)₂ capping group has a significant affect on the branching in the polymer. As noted above, **8l,m** contain -CH(*p*-tolyl)₂ capping groups and produce polyethylene that contains ca. 100 branches/10³ C. In contrast, analogues **8n,o** contain -CH(*m*-xylyl)₂ groups and produce polymers with ca. 60 branches/10³ C. The two 2-Me groups of the *m*-xylyl units may hinder olefin rotation in a palladium hydride olefin intermediate, which would be required to generate a branch in the polymer, or may simply disfavor secondary alkyl species.

The catalyst containing ligand **1q** gives the lowest polymer yield and molecular weight of the catalysts studied here, and the ethylene adduct **8q** was not observed. The extreme crowding in the (**1q**)PdR⁺ species inhibits ethylene coordination and growth.

Conclusion

The {RHC(heterocycle)₂}PdR⁺ system is an interesting platform for insertion polymerization catalyst development. (N[^]N)PdR⁺ species that contain sterically small (heterocycle)₂-CHR ligands (**1a,d-f**) are ethylene dimerization catalysts. Incorporation of bulky substituents in the bridging methylene position shifts the product distribution to higher molecular weights due to inhibition of chain transfer. In general, more electron-deficient and sterically crowded (N[^]N)Pd(R)-(ethylene)⁺ exhibit higher ethylene insertion rates.

(23) Since $X_n = R_{\text{growth}}/R_{\text{trans}}$, for two catalysts **A** and **B**, the ratio of chain transfer rates is given by $R_{\text{trans,A}}/R_{\text{trans,B}} = (R_{\text{growth,A}})(X_{n,B})/(R_{\text{growth,B}})(X_{n,A})$.

(24) (a) Camacho, D. H.; Salo, E. V.; Ziller, J. W.; Guan, Z. *Angew. Chem., Int. Ed.* **2004**, *43*, 1821. (b) Popeney, C.; Guan, Z. *Organometallics* **2005**, *24*, 1145. (c) Popeney, C.; Camacho, D. H.; Guan, Z. *J. Am. Chem. Soc.* **2007**, *129*, 10062.

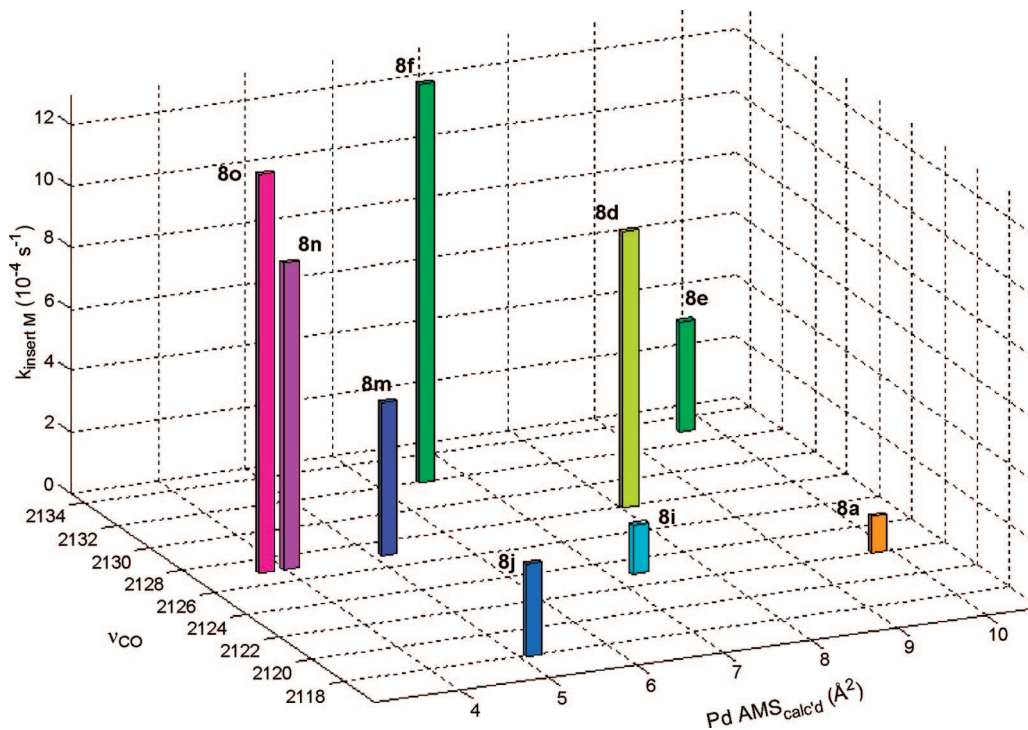


Figure 6. Dependence of the rate constant for ethylene insertion of $(N^{\wedge}N)PdMe(H_2C=CH_2)^+$ species ($k_{insert, Me}$, -10 °C, CD_2Cl_2 solution) on the Pd–CO ν_{CO} value for the corresponding $(N^{\wedge}N)Pd\{C(=O)Me\}CO^+$ species (ν_{CO}) and the calculated accessible molecular surface at Pd for the $(N^{\wedge}N)Pd$ unit (AMS).

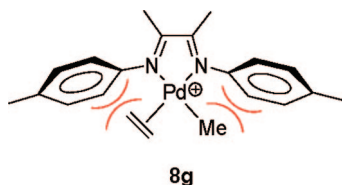


Figure 7. Steric interactions in complex **8g**.

Experimental Section

General Procedures. All manipulations were performed under nitrogen or vacuum using Schlenk or high-vacuum techniques or in a nitrogen-filled drybox. Nitrogen was purified by passage through columns containing activated molecular sieves and Q-5 oxygen scavenger. Pentane, hexanes, toluene, and benzene were purified by passage through columns of activated alumina and BASF R3-11 oxygen scavenger. Diethyl ether and tetrahydrofuran were distilled from Na/benzophenone ketyl. Dichloromethane was refluxed over CaH_2 and distilled. $CDCl_3$ and CD_2Cl_2 were dried over CaH_2 , degassed by freeze–pump–thaw cycles, and vacuum transferred to a storage vessel. Acetone- d_6 was dried over 4 Å molecular sieves. CO (Aldrich), ethylene (Matheson, research grade), $[HNMe_2Ph][B(C_6F_5)_4]$ and $[Li(Et_2O)_{2.8}][B(C_6F_5)_4]$ (Boulder Scientific), and $(cod)PdCl_2$ and $(MeCN)_2PdCl_2$ (Strem) were used as received. The Et_2O content of the $[Li(Et_2O)_{2.8}][B(C_6F_5)_4]$ salt was determined by 1H NMR with C_6Me_6 as internal standard. The compounds $(mim)_2CH_2$,²⁵ $[((4-Me-C_6H_4)_3C)HC(mim)_2]PdMe(NMe_2Ph)[B(C_6F_5)_4]$ (**5j**),¹⁶ $(cod)Pd(Me)Cl$,²⁶ $(pyridazine)PdMe_2$,²⁷ $[H(Et_2O)_2][B(C_6F_5)_4]$,²⁸ and $Tl[B(C_6F_5)_4]$ ²⁹ were prepared by literature procedures.

(25) Braussaud, N.; Ruther, T.; Cavell, K. J.; Skelton, B. W.; White, A. H. *Synthesis* **2001**, 626.

(26) Rülke, R. E.; Ernsting, J. M.; Spek, A. L.; Elsevier, C. J.; van Leeuwen, P. W. N. M.; Vrieze, K. *Inorg. Chem.* **1993**, 32, 5769.

(27) Byers, P. K.; Canty, A. J. *Organometallics* **1990**, 9, 210.

(28) Jutzi, P.; Mueller, C.; Stammler, A.; Stammler, H.-G. *Organometallics* **2000**, 19, 1442.

Elemental analyses were performed by Midwest Microlabs (Indianapolis, IN). Infrared spectra were obtained using a Nicolet NEXUS 470 FT-IR spectrometer. GC-MS analyses were performed on a HP-6890 instrument equipped with a HP-5973 mass selective detector.

NMR spectra were recorded in flame-sealed or Teflon-valved tubes on Bruker AMX-400 or AMX-500 spectrometers at ambient probe temperature unless otherwise indicated. 1H and ^{13}C chemical shifts are reported versus $SiMe_4$ and were determined by reference to the residual 1H and ^{13}C solvent peaks. ^{19}F and ^{11}B chemical shifts were referenced to external neat $CFCl_3$ and $BF_3 \cdot Et_2O$, respectively. Coupling constants are reported in Hz. NMR probe temperatures were calibrated by a MeOH thermometer.³⁰

The NMR spectra of cationic Pd compounds contained signals of the free $B(C_6F_5)_4^-$ anion. $^{13}C\{^1H\}$ NMR (CD_2Cl_2 , -60 °C): δ 147.5 (dm, $J = 241$, C2), 137.8 (dm, $J = 238$, C4), 135.8 (dm, $J = 249$, C3), 123.6 (br, C1). ^{11}B NMR (CD_2Cl_2 , -60 °C): δ -16.9 (s). ^{19}F NMR (CD_2Cl_2 , -60 °C): δ -133.7 (br s, 2F, *o*-F), -163.0 (t, $J = 23$, 1F, *p*-F), -167.0 (t, $J = 19$, 2F, *m*-F). NMR spectra of **7i,j** and **8i,j** and species derived from these species contain resonances for free NMe_2Ph .³¹ Solutions of cationic species generated in situ from the reaction of **3l–o** and $[Li(Et_2O)_{2.8}][B(C_6F_5)_4]$ contain LiCl. Solutions of cationic species generated in situ from the reaction of **3q** and $Tl[B(C_6F_5)_4]$ contain TlCl. The cationic Pd compounds were not isolated due to their thermal instability and were characterized by NMR.

(29) Alberti, D.; Poerschke, K.-R. *Organometallics* **2004**, 23, 1459.

(30) Van Geet, A. L. *Anal. Chem.* **1970**, 42, 679.

(31) (a) Data for free NMe_2Ph : 1H NMR (CD_2Cl_2): δ 7.20 (m, 2H, *o*-Ph), 6.72 (m, 2H, *m*-Ph), 6.67 (t, $J = 7$, 1H, *p*-Ph), 3.03 (s, 6H, Me). $^{13}C\{^1H\}$ NMR (CD_2Cl_2): δ 151.1 (C1), 129.3 (C2), 116.6 (C4), 112.8 (C3), 40.7 (Me). 1H NMR (CD_2Cl_2 , -60 °C): δ 7.18 (m, 2H, *o*-Ph), 6.67 (m, 2H, *m*-Ph), 6.63 (t, $J = 7$, 1H, *p*-Ph), 2.88 (s, 6H, Me). $^{13}C\{^1H\}$ NMR (CD_2Cl_2 , -60 °C): δ 150.2 (C1), 128.7 (C2), 115.8 (C4), 111.9 (C3), 40.3 (Me). (b) If excess $[HNMe_2Ph][B(C_6F_5)_4]$ is used in the generation of **5i** and **5j**, and the NMe_2Ph is then displaced from **5i** and **5j** by another ligand, the excess $HNMe_2Ph^+$ undergoes fast H^+ exchange with NMe_2Ph and a single set of $NMe_2Ph/HNMe_2Ph^+$ resonances at the weighted average of the chemical shifts of these species is observed.

Gel permeation chromatography was performed on a Polymer Laboratories PL-GPC 220 instrument using 1,2,4-trichlorobenzene solvent (stabilized with 125 ppm BHT) at 150 °C. A set of three PLgel 10 μ m Mixed-B or Mixed-B LS columns was used. Samples were prepared at 160 °C. Polyethylene molecular weights were determined by GPC versus polystyrene standards and are reported relative to polyethylene standards, as calculated by the universal calibration method using Mark-Houwink ($K = 14.1 \times 10^{-5}$, $\alpha = 0.70$ for polystyrene, $K = 40.6 \times 10^{-5}$, $\alpha = 0.725$ for polyethylene). Total branching of the polyethylenes was determined by ^1H NMR.³²

(mim)₂CH(CH(4-Me-C₆H₄)₂) (1i). A slurry of (mim)₂CH₂ (0.60 g, 3.4 mmol) in THF (60 mL) at -78 °C was prepared and $^n\text{BuLi}$ (2.26 M in hexanes, 1.66 mL, 3.74 mmol) was added over 5 min while the mixture was stirred. A deep yellow solution formed. The solution was stirred at -78 °C for 1.5 h, and a solution of (4-Me-C₆H₄)₂HCCl (0.86 g, 3.7 mmol) in THF (15 mL) was added via cannula. The mixture was stirred and warmed to 25 °C over 12 h. The volatiles were removed under vacuum, and the resulting tan residue was taken up in CH₂Cl₂ (200 mL) and H₂O (100 mL). The CH₂Cl₂ layer was separated and washed with aqueous Na₂CO₃, aqueous NaHCO₃, and H₂O and dried over MgSO₄. The volatiles were removed under vacuum to afford an off-white solid that contained the desired product and (4-Me-C₆H₄)₂HC-CH(4-Me-C₆H₄)₂. The mixture was separated by column chromatography using grade IV alumina and benzene (200 mL) followed by acetone (200 mL). The fractions were analyzed by UV-vis, and those that contained the product were combined and dried under vacuum. The product was dissolved in CH₂Cl₂ (100 mL), washed with H₂O (25 mL), dried over MgSO₄, and dried under vacuum to afford a white solid (0.86 g, 67%). ^1H NMR (CD₂Cl₂): δ 7.16 (d, 4H, $J = 8$, 4-Me-C₆H₄), 6.99 (d, 4H, $J = 8$, 4-Me-C₆H₄), 6.76 (s, 2H, mim H4), 6.59 (s, 2H, mim H5), 5.32 (d, $J = 12$, 1H, CH), 5.29 (d, $J = 12$, 1H, CH), 3.58 (s, 6H, NMe), 2.21 (s, 6H, 4-Me-C₆H₄). ^{13}C NMR (CD₂Cl₂): δ 145.9, 140.3, 136.3, 129.3, 128.1, 127.0, 121.6, 52.5, 43.2, 33.2, 20.9. Anal. Calcd for C₂₄H₂₆N₄: C, 77.80; H, 7.07; N, 15.13. Found: C, 77.51; H, 7.16; N, 14.93. GC-MS *m/z*: 370 (M⁺).

1j–q. These ligands were prepared using procedures analogous to that for **1i**. Details are given in the Supporting Information.

{((4-Me-C₆H₄)₂HC)HC(mim)₂}PdMe₂ (2i). A Et₂O (40 mL) solution of (mim)₂CH(CH(4-Me-C₆H₄)₂) (0.20 g, 0.55 mmol) was added via cannula to an Et₂O (10 mL) suspension of (pyridazine)PdMe₂ (0.11 g, 0.50 mmol). The mixture was stirred for 1 h at 25 °C and filtered to afford a white solid. The solid was rinsed with Et₂O. The solid was dissolved in 10 mL of CH₂Cl₂ at -78 °C. The resulting clear yellow solution was warmed to 0 °C, and the volatiles were removed under vacuum. The off-white solid that remained was washed thoroughly with pentane and dried under vacuum (0.16 g, 63%). ^1H NMR (CD₂Cl₂, -60 °C): δ 7.15 (d, 4H, $J = 8$, 4-Me-C₆H₄), 7.00 (d, 4H, $J = 8$, 4-Me-C₆H₄), 6.91 (s, 2H, mim H4/H5), 6.57 (s, 2H, mim H4/H5), 6.23 (d, $J = 12$, 1H, CH), 4.57 (d, $J = 12$, 1H, CH), 3.24 (s, 6H, NMe), 2.20 (s, 6H, 4-Me-C₆H₄), 0.07 (s, 6H, PdMe). ^{13}C NMR (CD₂Cl₂, -60 °C): δ 143.8, 136.7, 136.6, 128.8, 127.5, 125.9, 119.9, 57.0, 39.2, 33.2, 20.6, -10.4 (PdMe). **2i** was stored at -35 °C and is insufficiently stable for elemental analysis.

{((4-Me-C₆H₄)₃C)HC(mim)₂}PdMe₂ (2j). A Et₂O (25 mL) solution of (mim)₂CH(CH(4-Me-C₆H₄)₃) (0.25 g, 0.55 mmol) was added to an Et₂O (5 mL) suspension of (pyridazine)PdMe₂ (0.11 g, 0.50 mmol). The mixture was stirred for 1 h at 25 °C and filtered to afford a white solid. The solid was washed with Et₂O and dried under vacuum (0.23 g, 79%). ^1H NMR (CD₂Cl₂, -60 °C): δ 6.91 (d, 6H, $J = 8$, 4-Me-C₆H₄), 6.86 (s, 4H, mim H4/H5), 6.63 (s, 2H, mim H4/H5), 6.62 (d, 6H, $J = 8$, 4-Me-C₆H₄), 5.63 (s, 1H, CH), 3.10 (s, 6H, NMe), 2.27 (s, 9H, 4-Me-C₆H₄), -0.48 (s, 6H, PdMe).

$^{13}\text{C}\{^1\text{H}\}$ NMR (CD₂Cl₂, -60 °C): δ 142.3, 139.6, 136.3, 131.1, 127.3, 125.8, 120.8, 64.5, 44.2, 34.2, 20.4, -10.7 (PdMe). **2j** was stored at -35 °C and is insufficiently stable for elemental analysis.

{((2,4-Me₂-C₆H₃)₂HC)HC(3-Me-quin)}PdMe₂ (2q). A flask was charged with (pyridazine)PdMe₂ (0.090 g, 0.42 mmol) and (3-Me-quin)₂CH(CH(2,4-Me₂-C₆H₃)₂) (0.25 g, 0.465 mmol), and Et₂O (40 mL) was added. A yellow precipitate formed rapidly. The mixture was stirred at 23 °C for 45 min. The yellow solid was collected by filtration, rinsed with Et₂O, and dried under vacuum (0.25 g, 90%). The product contained 0.06 equiv of Et₂O, which was quantified by NMR. ^1H NMR (CD₂Cl₂, -20 °C): δ 9.11 (d, $J = 8$, 2H, quin H8), 8.65 (br s, 1H, CH), 7.89 (s, 2H, quin H4), 7.66 (d, $J = 8$, 2H, quin H5), 7.61 (m, 2H, quin H6/H7), 7.45 (m, 2H, quin H6/H7), 7.20 (d, $J = 8$, 2H, H6 of 2,4-Me₂-C₆H₃), 6.85 (d, $J = 8$, 2H, H5 of 2,4-Me₂-C₆H₃), 6.78 (s, 2H, H3 of 2,4-Me₂-C₆H₃), 5.96 (d, $J = 11$, 1H, CH), 2.4 (s, 6H, quin 3-Me), 2.17 (s, 6H, 4-Me of 2,4-Me₂-C₆H₃), 1.87 (s, 6H, 2-Me of 2,4-Me₂-C₆H₃), 0.08 (s, 6H, PdMe). $^{13}\text{C}\{^1\text{H}\}$ NMR (CD₂Cl₂, -20 °C): δ 159.9, 145.8, 138.7, 137.6, 137.4, 135.6, 131.6, 131.3, 131.2, 128.5, 127.7, 127.1, 126.7, 126.2, 125.9, 55.2, 47.9, 20.8, 20.7, 19.6, -5.6 (PdMe). **2q** was stored at -35 °C and is insufficiently stable for elemental analysis.

{((4-Me-C₆H₄)₂HC)HC(5-Me-py)₂}Pd(Me)Cl (3l). A flask was charged with (cod)Pd(Me)Cl (0.133 g, 0.500 mmol) and (5-Me-py)₂CH(CH(4-Me-C₆H₄)₂) (0.206 g, 0.524 mmol), and Et₂O (60 mL) was added. A white precipitate formed rapidly. The mixture was stirred at 23 °C for 2 h and filtered to afford a white solid. The solid was rinsed with Et₂O, washed thoroughly with pentane, and dried under vacuum (0.251 g, 91%). The product contained 0.14 equiv of Et₂O, which was quantified by NMR. Only the **3l**-H_{eq} conformer is present at room temperature in CD₂Cl₂ solution, but a 1/2 **3l**-H_{eq}/**3l**-H_{ax} mixture is present at -60 °C. ^1H NMR (CD₂Cl₂, **3l**-H_{eq}): δ 8.78 (s, 1H, py H6/H6'), 8.37 (s, 1H, py H6/H6'), 7.88 (d, $J = 12$, 1H, CH), 7.37 (m, 3H), 7.30 (d, $J = 8$, 2H, 4-Me-C₆H₄), 7.25 (br d, 1H, py H3/H3'), 7.16 (d, $J = 8$, 1H, py H4/4'), 7.00 (d, $J = 8$, 2H, 4-Me-C₆H₄), 6.95 (m, 3H), 4.92 (d, $J = 12$, 1H, CH), 2.21 (s, 3H, py 5-Me), 2.19 (s, 6H, 4-Me-C₆H₄), 2.17 (s, 3H, py 5'-Me), 0.94 (s, 3H, PdMe). $^{13}\text{C}\{^1\text{H}\}$ NMR (CD₂Cl₂, **3l**-H_{eq}): δ 155.8, 153.3, 152.7, 151.6, 139.1, 139.0, 138.7, 138.3, 136.6, 136.5, 134.1, 133.3, 129.6, 129.5, 128.4, 128.3, 127.3, 125.5, 61.4, 55.8, 21.0 (2C), 18.1, 18.0, -2.5 (PdMe). ^1H NMR (CD₂Cl₂, -60 °C, 1/2 mixture of **3l**-H_{eq}/**3l**-H_{ax}): key resonances of **3l**-H_{eq} δ 8.59 (s, 1H, py H6/H6'), 8.27 (s, 1H, py H6/H6'), 7.84 (d, $J = 12$, 1H, CH), 5.03 (d, $J = 12$, 1H, CH), 2.07 (s, 3H, py 5-Me), 1.93 (s, 3H, py 5'-Me), 0.86 (s, 3H, PdMe); key resonances **3l**-H_{ax} δ 8.48 (s, 1H, py H6/H6'), 8.24 (s, 1H, py H6/H6'), 6.41 (d, $J = 13$, 1H, CH), 5.10 (d, $J = 13$, 1H, CH), 2.13 (s, 3H, py 5-Me), 2.04 (s, 3H, py 5'-Me), 0.88 (s, 3H, PdMe); the other resonances of **3l**-H_{eq}/**3l**-H_{ax} are overlapped. Anal. Calcd for C₂₉H₃₁ClN₂Pd·0.14Et₂O: C, 63.42; H, 5.83; N, 5.00. Found: C, 63.17; H, 5.93; N, 5.16.

{((4-Me-C₆H₄)₂HC)HC(3-Me-py)₂}Pd(Me)Cl (3m). A flask was charged with (cod)Pd(Me)Cl (0.133 g, 0.500 mmol) and (3-Me-py)₂CH(CH(4-Me-C₆H₄)₂) (0.206 g, 0.524 mmol), and benzene (10 mL) was added by syringe. A white precipitate formed rapidly. The mixture was stirred at 23 °C for 1 h. Et₂O (5 mL) was added. The white solid was collected by filtration, rinsed with Et₂O and pentane, and dried under vacuum (0.185 g, 67%). The product contained 0.06 equiv of Et₂O and 0.01 equiv of C₆H₆, which were quantified by ^1H NMR. ^1H NMR (CD₂Cl₂): δ 8.92 (d, $J = 5$, 1H, py H6/H6'), 8.46 (d, $J = 12$, 1H, CH), 8.45 (d, $J = 5$, 1H, py H6/H6'), 7.45 (d, $J = 8$, 1H), 7.41 (d, $J = 8$, 2H, 4-Me-C₆H₄), 7.33 (m, 3H), 7.02 (m, 4H), 6.94 (d, $J = 8$, 2H, 4-Me-C₆H₄), 5.61 (d, $J = 12$, 1H, CH), 2.51 (s, 3H, Me), 2.24 (s, 3H, Me), 2.21 (s, 3H, Me), 2.19 (s, 3H, Me), 0.96 (s, 3H, PdMe). $^{13}\text{C}\{^1\text{H}\}$ NMR (CD₂Cl₂): δ 157.7, 155.1, 150.7, 149.7, 140.1, 139.7, 138.6, 138.5, 136.9, 136.8, 134.8, 133.5, 129.4, 129.2, 128.7, 128.6, 123.4, 122.9, 55.8, 51.7, 21.0 (2C), 20.8, 19.8, -2.2 (PdMe). Anal. Calcd for

$C_{29}H_{31}ClN_2Pd \cdot 0.06 Et_2O \cdot 0.01 C_6H_6$; C, 63.45; H, 5.75; N, 5.05. Found: C, 63.40; H, 5.81; N, 5.09.

{((2,4-Me₂-C₆H₃)₂HC)HC(5-Me-py)₂}Pd(Me)Cl (3n). A flask was charged with (cod)Pd(Me)Cl (0.133 g, 0.500 mmol) and (5-Me-py)₂CH(CH(2,4-Me₂-C₆H₃)₂) (0.231 g, 0.550 mmol), and benzene (10 mL) was added. A white precipitate formed rapidly. The mixture was stirred at 23 °C for 1.5 h. The white solid was collected by filtration, washed thoroughly with Et₂O and pentane, and dried under vacuum overnight (0.239 g, 83%). The isolated solid contained 0.03 equiv of C₅H₁₂, which was quantified by NMR. ¹H NMR (CD₂Cl₂, -66 °C): δ 8.71 (s, 1H, py H6'), 8.25 (s, 1H, py H6), 7.72 (d, *J* = 12, 1H, CH), 7.46 (m, 2H, H6/6' of 2,4-Me₂-C₆H₃ and py H4/4'), 7.39 (d, *J* = 8, 1H, H6/6' of 2,4-Me₂-C₆H₃), 7.32 (d, *J* = 8, 1H, py H3/H3'), 7.25 (d, *J* = 8, 1H, py H4/4'), 6.89 (m, 2H, H5/5' of 2,4-Me₂-C₆H₃), 6.80 (d, *J* = 8, 1H, py H3/H3'), 6.77 (s, 1H, H3' of 2,4-Me₂-C₆H₃), 6.67 (s, 1H, H3 of 2,4-Me₂-C₆H₃), 4.91 (d, *J* = 12, 1H, CH), 2.35 (s, 3H, 2-Me of 2,4-Me₂-C₆H₃), 2.18 (s, 3H, py 5-Me), 2.15 (s, 3H, py 5-Me), 2.14 (s, 3H, 2'-Me of 2,4-Me₂-C₆H₃), 2.12 (s, 3H, 4/4'-Me of 2,4-Me₂-C₆H₃), 2.10 (s, 3H, 4/4'-Me of 2,4-Me₂-C₆H₃), 0.74 (s, 3H, PdMe). Key ¹H-¹H NOESY correlations (-20 °C) δ/δ: 8.77 (py H6'/2.20 (py H5/H5'-Me); 8.29 (py H6/2.20 (py 5-Me); 8.29 (py H6)/0.79 (PdMe); 7.54 (CH)/2.39 (2-Me of 2,4-Me₂-C₆H₃); 7.54 (CH)/2.19 (2'-Me of 2,4-Me₂-C₆H₃); 7.32 (py H3)/4.91 (CH); 6.80 (py H3')/4.91 (CH); 2.39 (2-Me of 2,4-Me₂-C₆H₃)/0.79 (PdMe). ¹³C{¹H} NMR (CD₂Cl₂, -66 °C): δ 154.8, 152.2, 151.9, 150.5, 138.3, 138.0, 136.7, 136.5, 136.0, 135.4, 135.3, 133.8, 133.1, 131.0, 130.7, 127.8, 127.6, 126.3, 126.0, 125.1, 61.6, 45.4, 30.4, 20.3, 20.1, 17.8, 17.7, -2.4 (PdMe). Anal. Calcd for C₃₁H₃₅ClN₂Pd · 0.03 C₅H₁₂: C, 64.54; H, 6.15; N, 4.83. Found: C, 65.06; H, 6.55; N, 4.70.

{((2,4-Me₂-C₆H₃)₂HC)HC(3-Me-py)₂}Pd(Me)Cl (3o). A flask was charged with (cod)Pd(Me)Cl (0.133 g, 0.500 mmol) and (3-Me-py)₂CH(CH(2,4-Me₂-C₆H₃)₂) (0.220 g, 0.524 mmol), and benzene (15 mL) was added. The solution was stirred at 23 °C for 2 h. The volatiles were removed under vacuum to yield a white solid, which was washed thoroughly with Et₂O, rinsed with pentane, and dried under vacuum (0.243 g, 82%). The product contained 0.16 equiv of C₅H₁₂, which was quantified by NMR. ¹H NMR (CD₂Cl₂): δ 8.90 (d, *J* = 5, 1H, py H6'), 8.31 (d, *J* = 5, 1H, py H6), 8.04 (d, *J* = 11, 1H, CH), 7.57 (d, *J* = 8, 1H, py H4), 7.39 (d, *J* = 8, 1H, py H4'), 7.30 (d, *J* = 8, 1H, H6 of 2,4-Me₂-C₆H₃), 7.10 (m, 1H, py H5'), 7.03 (m, 2H, py H5 and H6' of 2,4-Me₂-C₆H₃), 6.89 (d, *J* = 8, 1H, H5 of 2,4-Me₂-C₆H₃), 6.85 (s, 1H, H3 of 2,4-Me₂-C₆H₃), 6.78 (m, 2H, H5' and H3' of 2,4-Me₂-C₆H₃), 5.51 (d, *J* = 11, 1H, CH), 2.57 (s, 3H, py 3-Me), 2.39 (s, 3H, 2-Me of 2,4-Me₂-C₆H₃), 2.19 (s, 3H, 4-Me of 2,4-Me₂-C₆H₃), 2.17 (s, 3H, 4'-Me of 2,4-Me₂-C₆H₃), 1.92 (s, 3H, 2'-Me of 2,4-Me₂-C₆H₃), 1.88 (s, 3H, py 3'-Me), 0.73 (s, 3H, PdMe). Key ¹H-¹H NOESY correlations (-20 °C) δ/δ: 8.84 (py H6')/1.84 (2'-Me of 2,4-Me₂-C₆H₃); 8.26 (py H6)/0.66 (PdMe); 7.99 (CH)/2.36 (2-Me of 2,4-Me₂-C₆H₃); 7.99 (CH)/1.84 (2'-Me of 2,4-Me₂-C₆H₃); 5.45 (CH)/2.57 (py 3-Me); 5.45 (CH)/1.83 (py 3'-Me); 2.35 (2-Me of 2,4-Me₂-C₆H₃)/0.66 (PdMe). ¹³C{¹H} NMR (CD₂Cl₂): δ 158.7, 155.3, 150.3, 149.9, 140.1, 139.8, 137.8, 137.7, 137.1, 136.3, 135.9, 134.9, 134.0, 131.9, 131.5, 129.4, 127.5, 126.9, 126.0, 123.2, 123.2, 52.9, 48.1, 20.9, 20.6, 19.7, 19.0, -2.2 (PdMe). Anal. Calcd for C₃₁H₃₅ClN₂Pd · 0.16 C₅H₁₂: C, 64.84; H, 6.32; N, 4.76. Found: C, 65.31; H, 6.57; N, 4.76.

{((2,4-Me₂-C₆H₃)₂HC)HC(3-Me-quin)₂}Pd(Me)Cl (3q). A flask was charged with (cod)Pd(Me)Cl (0.051 g, 0.193 mmol) and (3-Me-quin)₂CH(CH(2,4-Me₂-C₆H₃)₂) (0.125 g, 0.232 mmol), and Et₂O (20 mL) was added. A white precipitate formed rapidly. The mixture was stirred at 23 °C for 1 h. The solid was collected by filtration, rinsed with Et₂O, and dried under vacuum (0.070 g, 54%). The product contained 0.13 equiv of Et₂O, which was quantified by NMR. ¹H NMR (CD₂Cl₂, -60 °C): δ 9.31 (d, *J* = 9, 1H, quin H8/H8'), 9.03 (d, *J* = 9, 1H, quin H8/H8'), 8.56 (d, *J* = 10, 1H,

CH), 8.09 (s, 1H, quin H4/H4'), 7.85 (s, 1H, quin H4/H4'), 7.68 (m, 4H), 7.49 (m, 2H), 7.33 (d, *J* = 8, 1H), 7.12 (d, *J* = 8, 1H), 6.97 (d, *J* = 8, 1H), 6.83 (s, 1H, H3/H3' of 2,4-Me₂-C₆H₃), 6.76 (d, *J* = 8, 1H), 6.75 (s, 1H, H3/H3' of 2,4-Me₂-C₆H₃), 5.98 (d, *J* = 10, 1H, CH), 2.87 (s, 3H, quin 3/3'-Me), 2.24 (s, 3H, 2'-Me of 2,4-Me₂-C₆H₃), 2.20 (s, 3H, 4/4'-Me of 2,4-Me₂-C₆H₃), 2.10 (s, 3H, 4/4'-Me of 2,4-Me₂-C₆H₃), 1.79 (s, 3H, quin 3/3'-Me), 1.55 (s, 3H, 2-Me of 2,4-Me₂-C₆H₃), 0.40 (s, 3H, PdMe). ¹³C{¹H} NMR (CD₂Cl₂, -60 °C): δ 161.4, 157.9, 145.2, 138.8, 138.2, 137.6, 137.5, 137.4, 136.9, 136.0, 135.4, 131.7, 131.5, 131.4, 131.2, 131.0, 130.2, 129.3, 129.0, 128.7, 127.5, 127.4, 127.3, 127.0, 126.8, 126.6, 126.4, 125.3, 55.4, 49.4, 22.0, 20.5, 20.4, 19.9, 19.2, 19.0, -4.1 (PdMe). Anal. Calcd for C₃₉H₃₉ClN₂Pd · 0.13 Et₂O: C, 69.07; H, 5.91; N, 4.08. Found: C, 69.17; H, 5.97; N, 4.04.

{((4-Me-C₆H₄)₂HC)HC(mim)₂}PdCl₂ (4i). A solution of (cod)PdCl₂ (0.429 g, 1.50 mmol) and (mim)₂CH(CH(4-Me-C₆H₄)₂) (0.584 g, 1.58 mmol) in CH₂Cl₂ (50 mL) was stirred for 1 h at 25 °C and evacuated to dryness. The resulting orange solid was washed thoroughly with Et₂O and then pentane and dried under vacuum (0.801 g, 97%). ¹H NMR (CD₂Cl₂): δ 7.38 (d, *J* = 1, 2H, mim H4), 7.36 (d, *J* = 8, 4H, 4-Me-C₆H₄), 7.11 (d, 4H, *J* = 8, 4-Me-C₆H₄), 6.57 (d, *J* = 1, 2H, mim H5), 6.23 (d, *J* = 11, 1H, CH), 4.68 (d, *J* = 11, 1H, CH), 3.26 (s, 6H, mim NMe), 2.28 (s, 6H, 4-Me-C₆H₄). Key ¹H-¹H NOESY correlation δ/δ: 4.68 (mim₂CH)/3.26 (mim NMe). ¹³C{¹H} NMR (CD₂Cl₂): δ 142.9, 138.3 (mim C2), 135.9, 129.9, 129.0 (mim C4), 128.6, 120.7 (mim C5), 60.1 (CH), 41.5 (CH), 34.4 (mim NMe), 21.1.

{((4-Me-C₆H₄)₂HC)HC(3-Me-py)₂}PdCl₂ (4m). A solution of (cod)PdCl₂ (0.143 g, 0.500 mmol) and (3-Me-py)₂CH(CH(4-Me-C₆H₄)₂) (0.206 g, 0.524 mmol) in CH₂Cl₂ (20 mL) was stirred for 12 h at 25 °C and evacuated to dryness. The resulting orange solid was washed thoroughly with Et₂O and dried under vacuum (0.119 g, 58%). ¹H NMR (CD₂Cl₂): δ 8.97 (d, *J* = 6, 2H, py H6), 8.78 (d, *J* = 12, 1H, CH), 7.56 (d, *J* = 8, 4H, 4-Me-C₆H₄), 7.45 (d, *J* = 8, 2H, py H4), 7.06 (m, 2H, py H5), 7.03 (d, *J* = 8, 4H, 4-Me-C₆H₄), 5.73 (d, *J* = 12, 1H, CH), 2.36 (s, 6H, py 3-Me) 2.22 (s, 6H, 4-Me-C₆H₄). Key ¹H-¹H NOESY correlations δ/δ: 8.78 (CH)/7.56 (H2 of 4-Me-C₆H₄); 7.56 (H2 of 4-Me-C₆H₄)/2.36 (py 3-Me); 5.73 (CH)/7.56 (H2 of 4-Me-C₆H₄); 5.73 (CH)/2.36 (py 3-Me). ¹³C{¹H} NMR (CD₂Cl₂): δ 155.1, 152.5, 141.3, 137.5, 137.3, 134.7, 129.5, 128.8, 123.5, 57.4, 53.9, 21.0, 20.3. Anal. Calcd for C₂₈H₂₈Cl₂N₂Pd: C, 59.01; H, 4.95; N, 4.92. Found: C, 58.92; H, 5.00; N, 4.78.

{((2,4-Me₂-C₆H₃)₂HC)HC(5-Me-py)₂}PdCl₂ (4n). A solution of (cod)PdCl₂ (0.143 g, 0.500 mmol) and (3-Me-py)₂CH(CH(2,4-Me₂-C₆H₃)₂) (0.252 g, 0.600 mmol) in CH₂Cl₂ (25 mL) was stirred for 12 h at 25 °C and evacuated to dryness. The resulting orange solid was washed thoroughly with benzene, rinsed with Et₂O and pentane, and dried under vacuum. (0.289 g, 93%). The product contained 0.36 equiv of C₆H₆, which was quantified by NMR. ¹H NMR (CD₂Cl₂): δ 8.90 (s, 2H, py H6), 7.72 (d, *J* = 12, 1H, CH), 7.56 (d, *J* = 8, 2H, H6 of 2,4-Me₂-C₆H₃), 7.43 (d, *J* = 8, 2H, py H4), 7.07 (d, *J* = 8, 2H, py H3), 6.96 (d, *J* = 8, 2H, H5 of 2,4-Me₂-C₆H₃), 6.82 (s, 2H, H3 of 2,4-Me₂-C₆H₃), 5.06 (d, *J* = 12, 1H, CH), 2.42 (s, 6H, 2-Me of 2,4-Me₂-C₆H₃), 2.27 (s, 6H, py 5-Me), 2.19 (s, 6H, 4-Me of 2,4-Me₂-C₆H₃). Key ¹H-¹H NOESY correlations δ/δ: 8.90 (py H6)/2.42 (2-Me of 2,4-Me₂-C₆H₃), 7.72 (CH)/2.42 (2-Me of 2,4-Me₂-C₆H₃), 7.56 (H6 of 2,4-Me₂-C₆H₃)/7.07 (py H3); 7.07 (py H3)/5.06 (CH). ¹³C{¹H} NMR (CD₂Cl₂): δ 153.7, 152.8, 139.5, 137.3, 136.2, 135.9, 134.2, 131.6, 127.9, 126.7, 126.4, 51.0, 20.7, 20.5, 17.8. Anal. Calcd for C₃₀H₃₂Cl₂N₂Pd · 0.36 C₆H₆: C, 61.92; H, 5.52; N, 4.49. Found: C, 61.96; H, 5.59; N, 4.37.

{((2,4-Me₂-C₆H₃)₂HC)HC(3-Me-py)₂}PdCl₂ (4o). A solution of (cod)PdCl₂ (0.125 g, 0.437 mmol) and (3-Me-py)₂CH(CH(2,4-Me₂-C₆H₃)₂) (0.202 g, 0.480 mmol) in CH₂Cl₂ (25 mL) was stirred for 48 h at 25 °C. The orange mixture was filtered through a fine glass

frit and evacuated to dryness. The orange solid was washed thoroughly with Et₂O, rinsed with pentane, and dried under vacuum (0.209 g, 78%). The product contained 0.09 equiv of Et₂O and 0.12 equiv of C₅H₁₂, which were quantified by NMR. ¹H NMR (CDCl₃): δ 9.00 (d, *J* = 5, 2H, py H6), 8.31 (d, *J* = 11, 1H, CH), 7.51 (d, *J* = 8, 2H, py H4), 7.25 (d, *J* = 9, 2H, H6 of 2,4-Me₂-C₆H₃), 7.03 (m, 2H, py H5), 6.82 (m, 4H, H3 and H5 of 2,4-Me₂-C₆H₃), 5.63 (d, *J* = 11, 1H, CH), 2.32 (s, 6H, 2-Me of 2,4-Me₂-C₆H₃), 2.25 (s, 6H, py 3-Me), 2.15 (s, 6H, 4-Me of 2,4-Me₂-C₆H₃). Key ¹H-¹H NOESY correlations δ/δ: 9.00 (py H6)/2.32 (2-Me of 2,4-Me₂-C₆H₃), 8.31(CH)/2.32 (2-Me of 2,4-Me₂-C₆H₃)/2.25 (py 3-Me); 7.25 (H6 of 2,4-Me₂-C₆H₃)/5.63 (CH); 5.63 (CH)/2.25 (py 3-Me). ¹³C{¹H} NMR (CDCl₃): δ 155.5, 152.5, 140.9, 137.7, 136.2, 136.1, 134.3, 132.0, 127.7, 126.2, 123.3, 54.3, 49.2, 20.8, 20.5, 19.9. Anal. Calcd for C₃₀H₃₂Cl₂N₂Pd·0.09 Et₂O·0.12 C₅H₁₂: C, 60.64; H, 5.64; N, 4.57. Found: C, 60.85; H, 5.55; N, 4.52.

{(2,4-Me₂-C₆H₃)₂HC}HC(quin)₂PdCl₂ (4p). A solution of (cod)PdCl₂ (0.120 g, 0.420 mmol) and (quin)₂CH(CH(2,4-Me₂-C₆H₃)₂) (0.246 g, 0.500 mmol) in CH₂Cl₂ (20 mL) was stirred for 12 h at 25 °C and evacuated to dryness. The resulting orange solid was washed thoroughly with benzene, rinsed with Et₂O and pentane, and dried under vacuum, yielding a yellow powder (0.268 g, 95%). **4p** exists as an 86/14 **4p**-H_{eq}/**4p**-H_{ax} mixture in CD₂Cl₂ solution at 25 °C. ¹H NMR (CD₂Cl₂, 86/14 **4p**-H_{eq}/**4p**-H_{ax} conformers): **4p**-H_{eq} δ 9.70 (d, *J* = 9, 2H, quin H8), 8.52 (d, *J* = 11, 1H, CH), 8.10 (d, *J* = 8, 2H, quin H4), 7.87 (m, 2H, quin H7), 7.82 (d, *J* = 8, 2H, H6 of 2,4-Me₂-C₆H₃), 7.73 (d, *J* = 8, 2H, quin), 7.60 (m, 2H, quin H6), 7.40 (d, *J* = 8, 2H, quin H3), 7.04 (d, *J* = 8.0, 2H, H5 of 2,4-Me₂-C₆H₃), 6.84 (s, 2H, H3 of 2,4-Me₂-C₆H₃), 5.76 (d, *J* = 11, 1H, CH), 2.27 (s, 6H, 2-Me of 2,4-Me₂-C₆H₃), 2.22 (s, 6H, 4-Me of 2,4-Me₂-C₆H₃); key resonances of **4p**-H_{ax}: δ 9.53 (d, *J* = 9, 2H, quin H8), 9.14 (d, *J* = 12, 1H, CH), 8.08 (d, *J* = 9, 2H), 7.90 (m, 2H), 7.66 (d, *J* = 8, 2H), 7.54 (m, 2H), 5.72 (d, *J* = 12, 1H, CH), 2.83 (s, 6H, Me of 2,4-Me₂-C₆H₃), 2.18 (s, 6H, Me of 2,4-Me₂-C₆H₃); the other resonances are overlapped with those of **4p**-H_{eq}. Key ¹H-¹H NOESY correlations of **4p**-H_{eq}: δ/δ: 9.70 (quin H8)/2.27 (2-Me of 2,4-Me₂-C₆H₃), 8.52 (CH)/2.27 (2-Me of 2,4-Me₂-C₆H₃), 7.82 (H6 of 2,4-Me₂-C₆H₃)/5.76 (CH); 7.40 (quin H3)/5.76 (CH). Anal. Calcd for C₃₆H₃₂Cl₂N₂Pd: C, 64.54; H, 4.81; N, 4.18. Found: C, 64.55; H, 4.93; N, 4.13.

{(2,4-Me₂-C₆H₃)₂HC}HC(3-Me-quin)₂PdCl₂ (4q). A solution of (MeCN)₂PdCl₂ (0.050 g, 0.193 mmol) and (3-Me-quin)₂CH(CH(2,4-Me₂-C₆H₃)₂) (0.115 g, 0.212 mmol) in CH₂Cl₂ (20 mL) was stirred for 12 h at 25 °C and evacuated to dryness. The resulting orange solid was washed thoroughly with Et₂O and dried under vacuum (0.124 g, 93%). ¹H NMR (CD₂Cl₂): δ 9.70 (d, *J* = 9, 2H, quin H8), 9.01 (br d, *J* = 8, 1H, CH), 8.02 (s, 2H, quin H4), 7.80 (m, 2H, quin H7), 7.68 (d, *J* = 8, 2H, quin H5), 7.57 (m, 2H, quin H6), 7.40 (d, *J* = 8, 2H, H6 of 2,4-Me₂-C₆H₃), 6.94 (d, *J* = 8, 2H, H5 of 2,4-Me₂-C₆H₃), 6.88 (s, 2H, H3 of 2,4-Me₂-C₆H₃), 6.29 (d, *J* = 10, 1H, CH), 2.40 (s, 6H, quin 3-Me), 2.22 (s, 6H, 4-Me of 2,4-Me₂-C₆H₃), 2.14 (s, 6H, 2-Me of 2,4-Me₂-C₆H₃). Key ¹H-¹H NOESY correlations δ/δ: 9.01 (CH)/2.14 (2-Me of 2,4-Me₂-C₆H₃); 7.40 (H6 of 2,4-Me₂-C₆H₃)/2.40 (quin 3-Me); 7.40 (H6 of 2,4-Me₂-C₆H₃)/6.29 (CH); 6.29 (CH)/2.40 (quin 3-Me). ¹³C{¹H} NMR (CD₂Cl₂): δ 140.8, 138.4, 137.8, 136.8, 132.3, 132.0, 131.3, 130.3, 128.8, 128.5, 128.3 (br s), 128.3, 127.1, 126.9, 59.1, 51.8, 20.9, 20.7. Anal. Calcd for C₃₈H₃₆Cl₂N₂Pd: C, 65.38; H, 5.20; N, 4.01. Found: C, 64.97; H, 5.22; N, 4.01.

Generation of [((4-Me-C₆H₄)₂HC)HC(mim)₂]PdMe(NMe₂Ph)[B(C₆F₅)₄] (5i). A valved NMR tube was charged with {((4-Me-C₆H₄)₂HC)HC(mim)₂}PdMe₂ (8.2 mg, 16 μmol) and [HNMe₂Ph][B(C₆F₅)₄] (12 mg, 16 μmol), and CD₂Cl₂ (0.7 mL) was added by vacuum transfer at -78 °C. The tube was shaken at -78 °C until both solids dissolved. The tube was kept at -78 °C and transferred to an NMR probe that had been precooled to

-60 °C, and NMR spectra were recorded. Complete conversion to **5i** was observed. ¹H NMR (CD₂Cl₂, -60 °C): δ 7.88 (d, *J* = 8, 2H, *o*-Ph), 7.44 (t, *J* = 8, 2H, *m*-Ph), 7.30 (t, *J* = 8, 1H, *p*-Ph), 7.28 (d, *J* = 8, 2H, 4-Me-C₆H₄), 7.16 (d, *J* = 8, 2H, 4-Me-C₆H₄), 7.03 (d, 2H, *J* = 8, 4-Me-C₆H₄), 6.99 (d, 2H, *J* = 8, 4-Me-C₆H₄), 6.87 (s, 1H, mim H4/H5), 6.62 (s, 1H, mim H4/H5), 6.52 (d, *J* = 12, 1H, CH), 6.40 (s, 1H, mim H4/H5), 4.69 (s, 1H, mim H4), 4.66 (d, *J* = 12, 1H, CH), 3.44 (s, 3H, mim NMe), 3.24 (s, 3H, NMe), 3.07 (s, 3H, mim NMe), 2.82 (s, 3H, NMe), 2.25 (s, 3H, 4-Me-C₆H₄), 2.21 (s, 3H, 4-Me-C₆H₄), 1.04 (s, 3H, PdMe). ¹³C{¹H} NMR (CD₂Cl₂, -60 °C): δ 152.6, 144.3, 143.7, 137.65, 137.61, 136.0, 135.6, 129.5, 129.2, 127.4, 127.2, 127.1, 127.0, 125.7, 121.9, 121.2, 120.9, 57.5, 56.3, 50.4, 39.2, 33.9, 33.4, 20.6, 2.6 (PdMe).

Generation of [((4-Me-C₆H₄)₂HC)HC(mim)₂]PdMe(NMe₂Ph)[B(C₆F₅)₄] (5j). This compound was generated quantitatively from {((4-Me-C₆H₄)₂HC)HC(mim)₂}PdMe₂ and [HNMe₂Ph][B(C₆F₅)₄] using the procedure for **5i**. ¹H NMR (CD₂Cl₂, -60 °C): δ 7.84 (d, *J* = 8, 2H, *o*-Ph), 7.42 (t, *J* = 8, 2H, *m*-Ph), 7.29 (t, *J* = 8, 1H, *p*-Ph), 7.01 (br s, 6H, H_{aryl} of 4-Me-C₆H₄), 6.86 (s, 1H, mim H4/H5), 6.80 (s, 1H, mim H4/H5), 6.60 (br s, 6H, H_{aryl} of 4-Me-C₆H₄), 6.49 (s, 1H, mim H4/H5), 5.57 (s, 1H, CH), 5.23 (s, 1H, mim H4), 3.15 (s, 3H, mim NMe), 2.89 (s, 3H, mim NMe), 2.84 (s, 3H, NMe), 2.54 (s, 3H, NMe), 2.30 (s, 9H, 4-Me of 4-Me-C₆H₄), 0.29 (s, 3H, PdMe). ¹³C{¹H} NMR (CD₂Cl₂, -60 °C): δ 152.9, 143.1 (mim C2/C2'), 142.9 (mim C2/C2'), 137.5, 131.3, 129.2, 128.3, 128.0, 127.0, 124.9, 122.3, 122.2, 121.9, 64.4, 56.0 (NMe), 50.3 (NMe), 45.0 (CH), 36.1 (mim NMe), 33.7 (mim NMe), 20.5, 4.5 (PdMe).

Generation of [((2,4-Me₂-C₆H₃)₂HC)HC(3-Me-quin)₂]PdMe(NCMe)[B(C₆F₅)₄] (6q). A valved NMR tube was charged with {((*m*-xylyl)₂HC)HC(3-Me-quin)₂}PdMe₂ (5 mg, 8 μmol) and [H(Et₂O)₂][B(C₆F₅)₄] (6 mg, 8 μmol), and CD₂Cl₂ (0.7 mL) was added by vacuum transfer at -78 °C. The tube was vigorously shaken at -78 °C until both solids dissolved. The tube was cooled to -196 °C, and acetonitrile (8 equiv) was added by vacuum transfer. The tube was warmed to -78 °C and transferred to a precooled (-60 °C) NMR probe. NMR spectra showed that **6q** had formed quantitatively. The tube was evacuated to dryness at 23 °C. The tube was cooled to -78 °C, and CD₂Cl₂ (0.7 mL) was added by vacuum transfer. The tube was transferred to a precooled (-60 °C) NMR probe. NMR spectra showed that **6q** was present and that the excess acetonitrile had been removed. ¹H NMR (CD₂Cl₂, -60 °C): δ 8.68 (d, *J* = 9, 2H, quin H8/H8'), 8.16 (s, 1H, quin H4/H4'), 8.00 (s, 1H, quin H4/H4'), 7.97 (d, *J* = 10, 1H, CH), 7.74 (m, 4H), 7.56 (m, 2H), 7.27 (d, *J* = 8, 1H, H6' of 2,4-Me₂-C₆H₃), 7.18 (d, *J* = 8, 1H, H6 of 2,4-Me₂-C₆H₃), 6.98 (d, *J* = 8, 1H, H5' of 2,4-Me₂-C₆H₃), 6.84 (br s, 2H, H3 and H5 of 2,4-Me₂-C₆H₃), 6.77 (s, 1H, H3' of 2,4-Me₂-C₆H₃), 6.04 (d, *J* = 10, 1H, CH), 2.69 (s, 3H, quin 3/3'-Me), 2.29 (s, 3H, NCMe), 2.18 (s, 3H, 4'-Me of 2,4-Me₂-C₆H₃), 2.12 (s, 3H, 4-Me of 2,4-Me₂-C₆H₃), 2.00 (s, 6H, quin 3/3'-Me and 2-Me of 2,4-Me₂-C₆H₃), 1.59 (s, 3H, 2'-Me of 2,4-Me₂-C₆H₃), 0.70 (s, 3H, PdMe). The ¹H NMR assignments were confirmed by a NOESY experiment. ¹³C{¹H} NMR (CD₂Cl₂, -60 °C): δ 161.2, 158.1, 144.9, 140.4, 139.6, 136.6, 136.5, 136.3, 136.2, 135.8, 135.4, 132.3, 132.0, 131.6, 131.0, 130.3, 130.2, 129.9, 128.8, 128.1, 127.9, 127.6, 127.5, 127.4, 127.3, 127.1, 126.9, 126.4, 122.0, 55.4, 50.2, 21.4, 20.5, 20.4, 19.8, 19.5, 18.6, 3.73, -1.0.

Generation of [((4-Me-C₆H₄)₂HC)HC(mim)₂]Pd(C(=O)Me)(CO)[B(C₆F₅)₄] (7i). A solution of **5i** in CD₂Cl₂ was generated in a valved NMR tube as described above and cooled to -196 °C. The tube was exposed to CO (5 atm), sealed, warmed to -78 °C, and then briefly warmed to 0 °C and vigorously shaken. The tube was kept at -78 °C and transferred to a precooled (-40 °C) NMR probe, and NMR spectra were recorded. The ¹H NMR spectrum established that **7i** had formed quantitatively. ¹H NMR (CD₂Cl₂, -40 °C): δ 7.25 (d, *J* = 8, 2H, 4-Me-C₆H₄), 7.13 (d, *J* = 8, 2H, 4-Me-C₆H₄), 7.06 (d, *J* = 8, 2H, 4-Me-C₆H₄), 7.03 (d, *J* = 8, 2H,

4-Me-C₆H₄), 6.88 (s, 1H, mim H4/H5), 6.73 (s, 3H, mim H4/H5), 5.36 (d, *J* = 12, 1H, CH), 4.74 (d, *J* = 12, 1H, CH), 3.49 (s, 3H, mim NMe), 3.12 (s, 3H, mim NMe), 2.77 (s, 3H, COMe), 2.25 (s, 6H, 4-Me-C₆H₄). ¹³C{¹H} NMR (CD₂Cl₂, -40 °C): δ 217.4 (C(O)Me), 173.5 (PdCO), 144.8, 143.7, 138.4, 138.3, 135.0, 134.6, 129.7, 129.6, 127.8, 127.5, 127.3, 126.5, 122.3, 122.1, 61.4 (CH), 41.5 (COMe), 39.8 (CH), 34.6 (mim NMe), 33.6, (mim NMe), 20.7. IR (CD₂Cl₂, cm⁻¹): 2123 (ν_{CO}), 1736 (ν_{acyl}).

Generation of [(((4-Me-C₆H₄)₃CHC(mim)₂)Pd{C(=O)Me}(CO))[B(C₆F₅)₄] (7j). This compound was generated quantitatively from **2j**, [HNMe₂Ph][B(C₆F₅)₄], and CO using the procedure for **7i**. ¹H NMR (CD₂Cl₂, -40 °C): δ 7.08 (d, *J* = 8, 6H, 4-Me-C₆H₄), 6.89 (s, 1H, mim H4/H5), 6.85 (s, 1H, mim H4/H5), 6.81 (s, 1H, mim H4/H5), 6.78 (s, 1H, mim H4/H5), 6.53 (br s, 6H, 4-Me-C₆H₄), 5.70 (s, 1H, CH), 3.24 (s, 3H, mim NMe), 3.01 (s, 3H, mim NMe), 2.45 (s, 3H, COMe), 2.33 (s, 9H, 4-Me-C₆H₄). ¹³C{¹H} NMR (CD₂Cl₂, -40 °C): δ 219.9 (C(O)Me), 172.7 (PdCO), 144.1 (mim C2/C2'), 141.7 (mim C2/C2'), 138.2, 137.3, 131.8, 128.4, 127.7, 126.0, 124.0, 122.7, 65.8, 44.7 (CH), 41.7 (COMe), 36.1 (mim NMe), 34.2, (mim NMe), 20.5. IR (CD₂Cl₂, cm⁻¹): 2119 (ν_{CO}), 1728 (ν_{acyl}).

Generation of [(((4-Me-C₆H₄)₂HC)HC(3-Me-py)₂)Pd{C(=O)Me}(CO))[B(C₆F₅)₄] (7m). A valved NMR tube containing a CD₂Cl₂ (0.7 mL) solution of **3m** (16 mg, 30 μmol) and [Li(Et₂O)_{2.8}][B(C₆F₅)₄] (27 mg, 30 μmol) was cooled to -196 °C and exposed to CO (5 atm). The tube was sealed, warmed to -78 °C, and briefly warmed to 23 °C and vigorously shaken. A slurry of a fine white solid in a colorless supernatant was obtained. The tube was kept at -78 °C and transferred to a precooled (-40 °C) NMR probe, and NMR spectra were recorded. NMR spectra showed that **7m** had formed quantitatively. ¹H NMR (CD₂Cl₂, -40 °C): δ 8.33 (d, *J* = 5, 1H, py H6/H6'), 8.25 (d, *J* = 5, 1H, py H6/H6'), 7.71 (d, *J* = 8, 1H, py H4/H4'), 7.55 (d, *J* = 8, 1H, py H4/H4'), 7.29 (m, 1H, py H5/H5'), 7.21 (d, *J* = 8, 2H, 4-Me-C₆H₄), 7.18 (m, 1H, py H5/H5'), 7.04 (m, 4H, 4-Me-C₆H₄), 6.99 (d, *J* = 8, 2H, 4-Me-C₆H₄), 6.93 (d, *J* = 12, 1H, CH), 5.66 (d, *J* = 12, 1H, CH), 2.83 (s, 3H, C(=O)Me), 2.48 (s, 3H, Me), 2.23 (s, 3H, Me), 2.20 (s, 3H, Me), 2.19 (s, 3H, Me). ¹³C{¹H} NMR (CD₂Cl₂, -40 °C): δ 216.7 (C(O)Me), 172.8 (PdCO), 155.8, 154.9, 149.5, 148.7, 147.6, 146.8, 143.3, 142.4, 137.7, 137.6, 136.8, 136.5, 136.3, 136.2, 129.6, 129.4, 127.7, 127.5, 124.3, 124.2, 58.8 (CH), 50.4 (CH), 41.7 (COMe), 20.7, 20.5, 19.7. IR (CD₂Cl₂, cm⁻¹): 2127 (ν_{CO}), 1742 (ν_{acyl}).

Generation of [(((2,4-Me₂-C₆H₃)₂HC)HC(5-Me-py)₂)Pd{C(=O)Me}(CO))[B(C₆F₅)₄] (7n). This compound was generated quantitatively from **3n**, [Li(Et₂O)_{2.8}][B(C₆F₅)₄], and CO using the procedure for **7m**. ¹H NMR (CD₂Cl₂, -60 °C): δ 8.22 (s, 1H, py H6/H6'), 8.05 (s, 1H, py H6/H6'), 7.76 (s, 2H), 7.44 (d, *J* = 8, 1H), 7.40 (d, *J* = 7.9, 1H), 7.20 (d, *J* = 8, 1H), 6.95 (d, *J* = 8, 1H), 6.92 (d, *J* = 8, 1H), 6.89 (s, 1H), 6.74 (d, *J* = 8, 1H), 6.69 (s, 1H), 6.50 (d, *J* = 12, 1H, CH), 5.02 (d, *J* = 12, 1H, CH), 2.51 (s, 3H, C(=O)Me), 2.30 (s, 3H, Me), 2.26 (s, 3H, Me), 2.25 (s, 3H, Me), 2.14 (s, 3H, Me), 2.13 (s, 3H, Me), 1.88 (s, 3H, Me). ¹³C{¹H} NMR (CD₂Cl₂, -60 °C): δ 216.9 (C(O)Me), 172.7 (PdCO), 153.4, 152.8, 150.8, 148.8, 141.8, 141.1, 136.5, 136.4, 135.7, 135.5, 135.4, 135.1, 134.7, 134.6, 131.7, 130.7, 129.7, 128.0, 1127.5, 127.4, 127.0, 126.4, 61.3 (CH), 47.8 (CH), 50.0 (COMe), 20.6, 20.4, 20.3, 19.3, 17.9, 17.7. IR (CD₂Cl₂, cm⁻¹): 2127 (ν_{CO}), 1749 (ν_{acyl}).

Generation of [(((2,4-Me₂-C₆H₃)₂HC)HC(3-Me-py)₂)Pd{C(=O)Me}(CO))[B(C₆F₅)₄] (7o). This compound was generated quantitatively from **3o**, [Li(Et₂O)_{2.8}][B(C₆F₅)₄], and CO using the procedure for **7m**. ¹H NMR (CD₂Cl₂, -60 °C): δ 8.33 (d, *J* = 5, 1H, py H6/H6'), 8.12 (d, *J* = 5, 1H, py H6/H6'), 7.83 (d, *J* = 8, 1H), 7.57 (d, *J* = 8, 1H), 7.27 (m, 2H), 7.14 (d, *J* = 8, 1H), 6.95 (d, *J* = 8, 1H), 6.92 (s, 1H), 6.80 (m, 4H), 5.54 (d, *J* = 11, 1H, CH), 2.72 (s, 3H, C(=O)Me), 2.28 (s, 3H, Me), 2.26 (s, 3H, Me), 2.18 (s, 3H, Me), 2.13 (s, 3H, Me), 1.65 (s, 3H, Me), 1.58 (s, 3H,

Me). ¹³C{¹H} NMR (CD₂Cl₂, -60 °C): δ 217.4 (C(O)Me), 172.5 (PdCO), 156.8, 154.4, 149.5, 147.1, 143.3, 142.4, 136.9, 136.8, 136.7, 136.4, 135.7, 135.6, 135.1, 132.0, 130.9, 129.0, 127.6, 126.6, 126.5, 124.5, 124.2, 51.7 (CH), 49.5 (CH), 40.3 (COMe), 21.2, 20.6, 20.4, 20.3, 18.4, 18.3. IR (CD₂Cl₂, cm⁻¹): 2127 (ν_{CO}), 1750 (ν_{acyl}).

Generation of [(((2,4-Me₂-C₆H₃)₂HC)HC(3-Me-quin)₂)Pd{C(=O)Me}(CO))[B(C₆F₅)₄] (7q). A valved NMR tube containing a CD₂Cl₂ (0.7 mL) solution of {((2,4-Me₂-C₆H₃)₂HC)HC(3-Mequin)₂}PdMe₂ (5 mg, 8 μmol) and [H(Et₂O)₂][B(C₆F₅)₄] (6 mg, 8 μmol) was cooled to -196 °C, exposed to CO (5 atm), sealed, warmed to -78 °C, and then briefly warmed to 23 °C and vigorously shaken. The tube was kept at -78 °C and transferred to a precooled (-40 °C) NMR probe, and NMR spectra were recorded. NMR spectra showed that **7q** had formed quantitatively. ¹H NMR (CD₂Cl₂, -40 °C): δ 8.65 (d, *J* = 9, 1H, quin H8/H8'), 8.39 (d, *J* = 9, 1H), 8.35 (s, 1H, quin H4/H4'), 8.07 (s, 1H, quin H4/H4'), 7.85 (m, 4H), 7.65 (m, 2H), 7.26 (m, 2H), 7.12 (d, *J* = 10, 1H, CH), 7.02 (d, *J* = 8, 1H), 6.92 (m, 2H), 6.68 (s, 1H), 6.16 (d, *J* = 11, 1H, CH), 2.93 (s, 3H, quin 3/3'-Me), 2.22 (s, 3H, 4/4'-Me of 2,4-Me₂-C₆H₃), 2.15 (s, 3H, C(=O)Me), 2.12 (s, 3H, 4/4'-Me of 2,4-Me₂-C₆H₃), 1.89 (s, 3H, quin 3/3'-Me), 1.70 (s, 3H, 2/2'-Me of 2,4-Me₂-C₆H₃), 1.43 (s, 3H, 2/2'-Me of 2,4-Me₂-C₆H₃). The ¹H NMR assignments were confirmed by a NOESY experiment. ¹³C{¹H} NMR (CD₂Cl₂, -40 °C): δ 211.5 (C(O)Me), 172.7 (PdCO), 161.1, 158.8, 145.3, 144.6, 142.4, 141.2, 137.5, 137.3, 136.7, 136.0, 135.0, 133.2, 132.6, 132.5, 132.2, 131.8, 131.4, 129.3, 129.0, 128.8, 128.5, 128.3, 128.1, 127.7, 127.0, 126.9, 126.5, 54.9 (CH), 52.8 (CH), 39.4 (COMe), 22.0, 20.6, 20.5, 20.3, 19.1, 18.9. IR (CD₂Cl₂, cm⁻¹): 2126 (ν_{CO}).

Generation of [(((4-Me-C₆H₄)₂HC)HC(mim)₂)PdMe(H₂C=CH₂)[B(C₆F₅)₄] (8i). A solution of **5i** in CD₂Cl₂ in a valved NMR tube was generated as described above and cooled to -196 °C, and ethylene (ca. 4 equiv) was added by vacuum transfer. The tube was warmed to -78 °C and transferred to a precooled (-60 °C) NMR probe. NMR spectra established that **8i** had formed (100% versus NMe₂Ph). At -60 °C, exchange of bound and free ethylene is slow on the NMR time scale. ¹H NMR (CD₂Cl₂, -60 °C): δ 7.12 (d, *J* = 8, 2H, 4-Me-C₆H₄), 7.08 (d, *J* = 8, 4H, 4-Me-C₆H₄), 7.04 (d, *J* = 8, 2H, 4-Me-C₆H₄), 6.94 (s, 1H, mim H4/H5), 6.74 (s, 1H, mim H4/H5), 6.70 (s, 1H, mim H4/H5), 6.68 (s, 1H, mim H4/H5), 5.33 (d, *J* = 11, 1H, CH), 4.95 (m, 4H, H₂C=CH₂, AA'XX'), 4.71 (d, *J* = 11, 1H, CH), 3.33 (s, 3H, mim NMe), 3.29 (s, 3H, mim NMe), 2.21 (s, 3H, 4-Me-C₆H₄), 2.20 (s, 3H, 4-Me-C₆H₄), 0.76 (s, 3H, PdMe). ¹³C{¹H} NMR (CD₂Cl₂, -60 °C): δ 144.4 (mim C2/C2'), 143.1 (mim C2/C2'), 137.9, 137.8, 135.0, 134.9, 129.4, 129.3, 127.2, 127.1, 125.4, 123.9, 122.0, 121.3, 86.7 (H₂C=CH₂), 61.5 (CH), 39.8 (CH), 33.9 (mim NMe), 33.8 (mim NMe), 20.6, 6.9 (PdMe).

Generation of [(((4-Me-C₆H₄)₃CHC(mim)₂)PdMe(H₂C=CH₂)[B(C₆F₅)₄] (8j). This species was generated quantitatively from **5j** and ethylene (ca. 4 equiv) using the procedure for **8i** and characterized by NMR at -40 °C. At -40 °C, exchange of bound and free ethylene is slow on the NMR time scale. ¹H NMR (CD₂Cl₂, -40 °C): δ 7.01 (d, *J* = 8, 6H, 4-Me-C₆H₄), 6.88 (s, 2H, mim H4/H5), 6.84 (s, 1H, mim H4/H5), 6.60 (s, 1H, mim H4/H5), 6.49 (d, *J* = 8, 6H, 4-Me-C₆H₄), 5.76 (s, 1H, CH), 4.33 (m, 4H, H₂C=CH₂, AA'XX'), 3.23 (s, 3H, mim NMe), 3.10 (s, 3H, mim NMe), 2.30 (s, 9H, 4-Me-C₆H₄), 0.14 (s, 3H, PdMe). ¹³C{¹H} NMR (CD₂Cl₂, -40 °C): δ 143.1 (mim C2/C2'), 142.2 (mim C2/C2'), 137.8, 137.7, 131.4, 128.2, 125.8, 123.5, 123.3, 122.7, 85.8 (H₂C=CH₂), 67.5, 44.5 (CH), 33.6 (mim NMe), 34.7 (mim NMe), 20.5, 6.5 (PdMe).

Generation of [(((4-Me-C₆H₄)₂HC)HC(5-Me-py)₂)PdMe(H₂C=CH₂)[B(C₆F₅)₄] (8l). A valved NMR tube containing a CD₂Cl₂ (0.7 mL) solution of **3l** (11 mg, 20 μmol) and [Li(Et₂O)_{2.8}][B(C₆F₅)₄] (18 mg, 0.020 μmol) was cooled to -196

°C, and ethylene (ca. 8 equiv) was added by vacuum transfer. The tube was sealed, warmed to -78 °C, and transferred to a precooled (-40 °C) NMR probe. NMR spectra established that **8l** had formed (100% vs Et₂O). At -40 °C, exchange of bound and free ethylene is slow on the NMR time scale. At -40 °C, **8l** exists as a 2/3 mixture of **8l**-H_{eq} and **8l**-H_{ax} conformers. ¹H NMR (CD₂Cl₂, -40 °C, 2/3 **8l**-H_{eq}/**8l**-H_{ax}) δ key resonances of **8l**-H_{eq}: 8.20 (s, 1H, py H6/H6'), 7.79 (s, 1H, py H6/H6'), 6.44 (d, $J = 13$, 1H, CH), 5.10 (br m, 4H, H₂C=CH₂, AA'XX'), 0.92 (s, 3H, PdMe); the resonances of **8l**-H_{ax}: δ 8.11 (s, 1H, py H6/H6'), 7.92 (s, 1H, py H6/H6'), 6.24 (d, $J = 13$, 1H, CH), 5.10 (br m, 4H, H₂C=CH₂, AA'XX'), 5.07 (d, $J = 13$, 1H, CH), 0.93 (s, 3H, PdMe); the other resonances of the two isomers overlap. ¹³C{¹H} NMR (CD₂Cl₂, -40 °C, 2/3 **8l**-H_{eq}/**8l**-H_{ax}): δ 154.3, 153.5, 153.2, 152.7, 150.5, 149.7, 147.8, 147.2, 140.9, 140.7, 140.2, 138.3, 138.2, 137.3, 137.2, 137.1, 137.0, 136.9, 135.3, 135.2, 134.7, 130.1, 130.0, 129.7, 129.6, 127.4, 127.3, 127.1, 127.0, 126.6, 126.5, 123.4, 123.3, 101.2, 89.5, 88.6, 59.9, 59.1, 56.9, 47.7, 35.6, 20.6, 17.9, 17.8, 17.7, 17.6, 9.3, 8.9.

Generation of [(4-Me-C₆H₄)₂HC]HC(3-Me-py)₂PdMe(H₂C=CH₂)[B(C₆F₅)₄] (8m**).** This species was generated quantitatively from **3m**, [Li(Et₂O)_{2.8}][B(C₆F₅)₄], and ethylene (8 equiv) using the procedure for **8l**, except that the NMR spectra were recorded at -60 °C. At -60 °C, exchange of bound and free ethylene is slow on the NMR time scale. ¹H NMR (CD₂Cl₂, -60 °C): δ 8.26 (d, $J = 5$, 1H, py H6/H6'), 7.85 (d, $J = 5$, 1H, py H6/H6'), 7.63 (d, $J = 8$, 1H, py H4/H4'), 7.54 (d, $J = 8$, 1H, py H4/H4'), 7.23 (m, 1H, py H5/H5'), 7.18 (m, 1H, py H5/H5'), 7.10 (d, $J = 7$, 4H, 4-Me-C₆H₄), 7.01 (m, 4H, 4-Me-C₆H₄), 6.77 (d, $J = 12$, 1H, CH), 5.66 (d, $J = 12$, 1H, CH), 5.00 (m, 4H, H₂C=CH₂, AA'XX'), 2.45 (s, 3H, Me), 2.29 (s, 3H, Me), 2.18 (s, 3H, Me), 2.16 (s, 3H, Me), 0.89 (s, 3H, PdMe). ¹³C{¹H} NMR (CD₂Cl₂, -60 °C): δ 155.6, 154.7, 148.7, 145.0, 142.0, 141.4, 137.3, 137.2, 136.5, 136.3, 135.5, 134.9, 129.3, 127.2, 124.1, 124.0, 88.0 (br s, H₂C=CH₂), 59.3 (CH), 50.6 (CH), 20.6, 20.3, 19.9, 9.0 (PdMe).

Generation of [(2,4-Me₂-C₆H₃)₂HC]HC(5-Me-py)₂PdMe(H₂C=CH₂)[B(C₆F₅)₄] (8n**).** This species was generated quantitatively from **3n**, [Li(Et₂O)_{2.8}][B(C₆F₅)₄], and ethylene (17 equiv) using the procedure for **8l**, except that the tube was warmed to -50 °C for 6 h prior to NMR analysis at -60 °C. At -60 °C, exchange of bound and free ethylene is slow on the NMR time scale. ¹H NMR (CD₂Cl₂, -60 °C): δ 8.14 (s, 1H, py H6/H6'), 7.73 (s, 1H, py H6/H6'), 7.65 (d, $J = 8$, 1H, py H), 7.51 (d, $J = 8$, 1H, py H), 7.39 (d, $J = 8$, 1H, H_{aryl} of 2,4-Me₂-C₆H₃), 7.35 (d, $J = 8$, 1H, H_{aryl} of 2,4-Me₂-C₆H₃), 7.29 (d, $J = 8$, 1H, H_{aryl} of 2,4-Me₂-C₆H₃), 7.03 (d, $J = 8$, 1H, H_{aryl} of 2,4-Me₂-C₆H₃), 6.93 (d, $J = 8$, 1H, py H), 6.88 (d, $J = 8$, 1H, py H), 6.77 (s, 1H, H6/H6' of 2,4-Me₂-C₆H₃), 6.75 (s, 1H, H6/H6' of 2,4-Me₂-C₆H₃), 6.26 (d, $J = 12$, 1H, CH), 4.98 (m, 4H, H₂C=CH₂, AA'XX'), 4.97 (d, $J = 12$, 1H, CH), 2.27 (s, 3H, Me), 2.25 (s, 3H, Me), 2.14 (s, 3H, Me), 2.12 (s, 3H, Me), 2.04 (s, 3H, Me), 1.90 (s, 3H, Me), 0.77 (s, 3H, PdMe). ¹³C{¹H} NMR (CD₂Cl₂, -60 °C): δ 153.9, 153.0, 150.3, 146.9, 140.7, 140.3, 136.3, 136.1, 135.4, 135.3, 135.2, 135.1, 135.0, 131.0, 130.9, 128.0, 127.3, 127.1, 126.5, 89.4 (br s, coord H₂C=CH₂), 62.1 (CH), 48.0 (CH), 20.4, 20.3, 20.1, 19.8, 17.9, 17.8, 9.2 (PdMe).

Generation of [(2,4-Me₂-C₆H₃)₂HC]HC(3-Me-py)₂PdMe(H₂C=CH₂)[B(C₆F₅)₄] (8o**).** This species was generated quantitatively from **3o**, [Li(Et₂O)_{2.8}][B(C₆F₅)₄], and ethylene (13 equiv) using the procedure for **8l**, except that the tube was warmed to -45 °C for 6 h prior to NMR analysis at -60 °C. NMR spectra showed that **8o** had formed (94% vs Et₂O) and trace ethylene insertion (6%) had occurred. At -60 °C, exchange of bound and free ethylene is slow on the NMR chemical shift time scale. ¹H NMR (CD₂Cl₂, -60 °C): δ 8.15 (d, $J = 5$, 1H, py H6/H6'), 7.78 (d, $J = 5$, 1H, py H6/H6'), 7.74 (d, $J = 8$, 1H, py H4/H4'), 7.59 (d, $J = 8$, 1H, py H4/H4'), 7.25 (m, 2H, py H5/H5'), 7.14 (d, $J =$

8, 1H, H_{aryl} of 2,4-Me₂-C₆H₃), 6.91 (d, $J = 8$, 1H, H_{aryl} of 2,4-Me₂-C₆H₃), 6.86 (d, $J = 8$, 1H, H_{aryl} of 2,4-Me₂-C₆H₃), 6.81 (m, 3H, H_{aryl} of 2,4-Me₂-C₆H₃), 6.52 (d, $J = 11$, 1H, CH), 5.50 (d, $J = 11$, 1H, CH), 4.87 (m, 4H, H₂C=CH₂, AA'XX'), 2.46 (s, 3H, Me), 2.18 (s, 3H, Me), 2.14 (s, 3H, Me), 2.00 (s, 3H, Me), 1.89 (s, 3H, Me), 1.72 (s, 3H, Me), 0.66 (s, 3H, PdMe). ¹³C{¹H} NMR (CD₂Cl₂, -60 °C): δ 155.6, 154.7, 148.7, 145.0, 142.0, 141.4, 137.3, 137.2, 136.5, 136.3, 135.5, 134.9, 129.3, 127.2, 124.1, 124.0, 88.6 (br s, H₂C=CH₂), 59.8 (CH), 49.5 (CH), 20.6, 20.3, 20.1, 19.9, 17.8, 17.6, 9.0 (PdMe).

Kinetics of Insertion of [(N[^]N)PdMe(H₂C=CH₂)] [B(C₆F₅)₄] Species (8i**, **j**, **l**–**o**).** The first-order rate constants ($k_{\text{insert,Me}}$) for the insertion of ethylene into the Pd–Me bond of (N[^]N)-PdMe(H₂C=CH₂)⁺ species **8i**, **j**, **l**–**o** were determined by ¹H NMR. The procedure for **8i** is described here. Analogous procedures were used for **8j**, **l**–**o**. Details and kinetic plots are provided in the Supporting Information. **Procedure for 8i:** A CD₂Cl₂ solution of **8i** containing 10 equiv of excess free ethylene was generated in a valved NMR tube as described above. The NMR tube was placed in a -10 °C constant-temperature bath for 20 min, placed in a -78 °C bath for 3 min, and transferred to a precooled (-60 °C) NMR probe, and a ¹H NMR spectrum was recorded at -60 °C. Values of $I_{0,\text{PdMe}}$, I_{PdMe} , and $I_{\text{NMe}_2\text{Ph}}$, where $I_{0,\text{PdMe}}$ = the integral of the Pd–Me resonance of **8i** ($\delta = 0.77$) at the start of the experiment, I_{PdMe} = the integral of the Pd–Me resonance of **8i** at the end of each 20 min interval, and $I_{\text{NMe}_2\text{Ph}}$ = the integral of the NMe₂Ph resonance ($\delta = 2.90$), were determined by careful integration of each spectrum. A plot of $\ln(A_{\text{PdMe}}/A_{0,\text{PdMe}})$, where $A_{\text{PdMe}} = I_{\text{PdMe}}/I_{\text{NMe}_2\text{Ph}}$ and $A_{0,\text{PdMe}} = I_{0,\text{PdMe}}/I_{\text{NMe}_2\text{Ph}}$ versus time was linear ($r^2 = 0.991$). The slope of this line equals $-k_{\text{insert,Me}}$. For **8i**, $k_{\text{insert,Me}} = (1.6 \pm 0.1) \times 10^{-4} \text{ s}^{-1}$ at -10 °C (~ 3 half-lives).

Ethylene Polymerization by (N[^]N)PdMe(L)⁺ Species in CH₂Cl₂. The following general procedure was used. Polymerizations were performed in a 200 mL Fischer-Porter bottle equipped with a magnetic stir bar, a stainless steel pressure head with inlet and outlet needle valves, a septum-capped ball valve for injections, a check valve for safety, and a pressure gauge. In a glovebox, the bottle was charged with the catalyst precursors (N[^]N)PdMe₂ complex **2** (30 μmol) and [HNMe₂Ph][B(C₆F₅)₄] (30 μmol), or (N[^]N)PdMeCl complex **3** (30 μmol) and [Li(Et₂O)_{2.8}][B(C₆F₅)₄] (30 μmol), or complex **3** (30 μmol) and Ti[B(C₆F₅)₄] and sealed. The bottle was removed from the glovebox and attached to a stainless steel double-manifold vacuum/ethylene line. The nitrogen atmosphere was removed by vacuum, and the bottle flushed with ethylene (3 atm). The bottle was cooled (-65 °C) and vented to decrease the ethylene pressure to 1 atm, and CH₂Cl₂ (20 mL) was added by syringe. The bottle was sealed, and the ethylene pressure was immediately increased to the experimental pressure (3 atm). The solution was stirred at -40 °C for 30 min, warmed to 25 °C, and stirred for 18 h. The pressure was kept constant by feeding ethylene on demand. The reaction mixture was initially a pale yellow but turned black as the polymerization proceeded, indicating the formation of Pd⁰. The polymerization was terminated by venting the reaction vessel and addition of excess methanol (50–100 mL). The volatiles were removed under vacuum, the residue was dissolved in hexanes (200 mL), and the solution was filtered through a plug of silica gel to give a solution that appeared clear and almost colorless. The solvent was removed, and the polymer oil was dried under vacuum for several days.

Ethylene Polymerization by (N[^]N)PdMe(L)⁺ Species in C₆H₅Cl. The procedure described above was used except for a slight difference in activation protocol. The bottle was charged with the catalyst precursors, flushed with ethylene (3 atm), and then cooled to -40 °C. The bottle was vented to decrease the ethylene pressure to 1 atm, C₆H₅Cl (20 mL) was added by syringe, the bottle was sealed, and the ethylene pressure was immediately increased to the experimental pressure (3 atm). The mixture was stirred at -35 °C

Table 6. Summary of X-Ray Diffraction Data for **4i**·C₂D₂Cl₄, **4n**·CHCl₃, **4o**·(2CHCl₃), and **4q**·(2.5CHCl₃)

	4i ·C ₂ D ₂ Cl ₄	4n ·CHCl ₃	4o ·2CHCl ₃	4q ·2.5CHCl ₃
formula	C ₂₄ H ₂₆ Cl ₂ N ₄ Pd + C ₂ D ₂ Cl ₄	C ₃₀ H ₃₂ Cl ₂ N ₂ Pd + CHCl ₃	C ₃₁ H ₃₂ Cl ₂ N ₂ Pd + 2CHCl ₃	C ₃₈ H ₃₆ Cl ₂ N ₂ Pd + 2.5CHCl ₃
fw	717.64 (including solv.)	717.24 (including solv.)	848.62 (including solv.)	995.90 (including solv.)
cryst syst	monoclinic	monoclinic	triclinic	monoclinic
space group	<i>Cc</i>	<i>Cc</i>	<i>P</i> $\bar{1}$	<i>P2</i> ₁ / <i>c</i>
<i>a</i> (Å)	14.873(8)	19.916(5)	9.397(2)	15.494(3)
<i>b</i> (Å)	11.336(5)	8.403(2)	9.948(2)	13.882(3)
<i>c</i> (Å)	17.234(8)	19.238(5)	19.007(4)	21.230(4)
α (deg)			85.413(4)	
β (deg)	93.618(2)	98.870(4)	86.325(4)	113.31(1)
γ (deg)			85.283(4)	
<i>V</i> (Å ³)	2900(2)	3181.0(1)	1762.3(7)	4193.6(1)
<i>Z</i>	4	4	2	4
temperature (K)	100	100	100	100
cryst color, habit	pale yellow, brick	pale yellow, fragment	yellow, plate	yellow, plate
GOF on <i>F</i> ²	0.801	1.027	0.994	1.156
final <i>R</i> indices	<i>R</i> ₁ = 0.0286	<i>R</i> ₁ = 0.0233	<i>R</i> ₁ = 0.0284	<i>R</i> ₁ = 0.0596
(<i>I</i> > 2σ(<i>I</i>)) ^a	w <i>R</i> ₂ = 0.0737	w <i>R</i> ₂ = 0.0527	w <i>R</i> ₂ = 0.0644	w <i>R</i> ₂ = 0.1524
<i>R</i> indices	<i>R</i> ₁ = 0.0291	<i>R</i> ₁ = 0.0236	<i>R</i> ₁ = 0.0339	<i>R</i> ₁ = 0.0631
(all data) ^a	w <i>R</i> ₂ = 0.0742	w <i>R</i> ₂ = 0.0528	w <i>R</i> ₂ = 0.0659	w <i>R</i> ₂ = 0.1548

$$^a R_1 = \sum |F_o| - |F_c|/F_o; wR_2 = [\sum(w(F_o^2 - F_c^2)^2)/\sum(w(F_o^2)^2)]^{1/2}, \text{ where } w = q[\sigma^2(F_o^2) + (aP)^2 + bP]^{-1}.$$

for 1 h, warmed to 25 °C, and stirred for 18 h. The polymer was isolated as described above.

X-Ray Crystallography. Crystallographic data are summarized in Table 6. Details are provided in the Supporting Information. Data were collected on a Bruker Smart Apex diffractometer using Mo K α radiation (0.71073 Å). Non-hydrogen atoms were refined with anisotropic displacement coefficients. Hydrogen and deuterium atoms were included in the structure factor calculation at idealized positions and were allowed to ride on the neighboring atoms with relative isotropic displacement coefficients. Specific comments for each structure are as follows.

{((4-Me-C₆H₄)₂HC)HC(mim)₂}PdCl₂ (4i**).** Crystals of **4i** were obtained by slow diffusion of pentane into a concentrated C₂D₂Cl₄ solution at 23 °C. One C₂D₂Cl₄ molecule per molecule of **4i** was present. The C25 and C26 atoms of the solvent exhibited elongated thermal ellipsoids.

{((2,4-Me₂-C₆H₃)₂HC)HC(5-Me-py)₂}PdCl₂ (4n**).** Crystals of **4n** were obtained by slow diffusion of Et₂O into a concentrated CHCl₃ solution at 23 °C. One CHCl₃ molecule per molecule of **4n** was present. The atoms of the CHCl₃ molecule showed slight disorder with large displacement ellipsoids.

{((2,4-Me₂-C₆H₃)₂HC)HC(3-Mepy)₂}PdCl₂ (4o**).** Crystals of **4o** were obtained by slow diffusion of Et₂O into a concentrated CHCl₃

solution at 23 °C. Two CHCl₃ molecules per molecule of **4o** were present, one of which was disordered over two overlapping positions. The atoms of the two CHCl₃ molecules showed occupancy values very close to 0.5.

{((2,4-Me₂-C₆H₃)₂HC)HC(3-Me-quin)₂}PdCl₂ (4q**).** Crystals of **4q** were obtained by slow diffusion of pentane into a concentrated CHCl₃ solution at 23 °C. 2.5 CHCl₃ molecules per molecule of **4q** were present; two were well behaved, but the third was present at half-occupancy at a center of symmetry. The displacement ellipsoids for the half-occupancy CHCl₃ were elongated; no attempt was made to locate/assign an H atom to this CHCl₃.

Acknowledgment. This work was supported by the U.S. Department of Energy (DE-FG-02-00ER15036).

Supporting Information Available: Atom-labeling schemes for ligands, additional synthetic procedures and spectroscopic data, kinetic data, ethylene polymerization data, and NMR spectra of **2i**, **2j**, **2q**, **6q**, **5i**, **7i**, and **8i**. This material is available free of charge via the Internet at <http://pubs.acs.org>.

OM700768J